



TECHNICAL UNIVERSITY OF CRETE
SCHOOL OF ELECTRICAL AND COMPUTER ENGINEERING

Development of a 3D tracking sensor for biomedical applications

Diploma Thesis by

Dimitrios Pediaditis

Examination Committee:

Professor Konstantinos Balas (supervisor)

Professor Konstantinos C. Kalaitzakis

Dr Kortsalioudakis Nathanail

Chania 2020

Acknowledgements

I would like to thank Professor Konstantinos Balas for giving me the opportunity to work on this thesis and also for being supportive and helpful.

Deepest gratitude is also due to the members of the diploma committee, Professor Konstantinos Kalaitzakis and Dr Kortsalioudakis Nathanail for their participation in the presentation and evaluation of my diploma thesis

Special thanks to my friends and Chris Rossos for his invaluable assistance and support for the completion of the current work.

Last but not least, I would like to sincerely thank my family for their support during my studies at the Technical University of Crete.

Abstract

With technology advancing at such a rapid pace, it is no wonder that the developments in science and engineering are being integrated into the medical sector. Any new knowledge of living systems gained through analytical techniques based on engineering sciences contribute to the progress of medicine. This integration has given rise to the interdisciplinary field of biomedical and as a result, created the need to develop more applications at this field. Prominent breakthroughs in the biomedical field include life-saving and life-changing technology such as artificial organs, bio-sensors, prosthetics, surgical devices, pacemakers, EEGs, regenerative tissue growth, pharmaceutical drugs, kidney dialysis, to name a few. Many biomechanical analyses are also interested in the position tracking. The growing demand for low-cost, portable and durable sensors are driven by this type of application.

In this thesis, a low-cost, low power, portable and durable device was developed by using a sensor called Inertial Measurement Unit (IMU). This sensor contains of a 3-axis accelerometer, a 3-axis gyroscope and often a 3-axis magnetometer. An Inertial Measurement Unit cannot provide directly 3D coordinates thus a software was also developed that is capable of providing the displacement of the sensor in 3D coordinates. The motivation for this work was to construct a device with adequate accuracy, portable, with the lowest cost as possible that can be embedded in biomedical applications.

Table of Contents

- Acknowledgements 3**
- Abstract..... 4**
- Table of Contents..... 6**
- List of Figures..... 9**
- List of Tables 12**
- CHAPTER 1 13**
 - 1.1 Introduction..... 13
 - 1.2 Applicability and User requirement..... 14
 - 1.3 Background 16
- CHAPTER 2..... 17**
 - 2.1 Overview of other position sensors and technologies 17
 - 2.2 Position Sensors 18
 - 2.2.1 Potentiometers 18
 - 2.2.2 Magnetostrictive position sensors 19
 - 2.2.3 Encoder – magnetic 21
 - 2.2.4 Encoders – optical 22
 - 2.2.5 LVDT/RVDT..... 24
 - 2.2.6 Resonant inductive position sensing..... 25
 - 2.3 Other Related Technologies to Tracking Position..... 26
 - 2.3.1 The Basic Position Measuring Principles..... 26
 - 2.3.2 Positioning Methods..... 30

2.3.3 Techonologies	32
2.4 Comparison	45
CHAPTER 3.....	47
3.1 <i>The Proposed Sensor</i>	47
3.2 IMU.....	47
3.2.1 Accelerometer.....	48
3.2.2 Gyroscope.....	52
3.2.3 Magnetometer	54
3.3 Orientation.....	54
3.3.1 Rotation matrices	55
3.3.2 Euler angles	55
3.3.3 Unit Quaternions	58
3.4 Position.....	61
3.5 <i>Hardware Implementation</i>	62
3.5.1 Arduino	62
3.5.2 MPU9250	63
3.5.3 I2C protocol	64
3.5.4 Our circuit.....	65
3.5.5 Unused hardware	66
3.6 <i>Software Implementation</i>	66
3.6.1 AHRS	67
3.6.2 Algorithm we used	70
CHAPTER 4.....	74
4.1 <i>Experimental results</i>	74
4.2 <i>Accuracy and Repeatability</i>	80
Chapter 5	86
<i>Conclusions and Future Work</i>	86
Bibliography.....	88

List of Figures

Figure 1 size of a MEMS	16
Figure 2 Potentiometer sensor	18
Figure 3 Magnetostrictive sensor	19
Figure 4 Magnetic encoder.....	21
Figure 5 Optical encoder	22
Figure 6 Linear Variable Differential Transformer sensor	24
Figure 7 Inductive position sensor for linear and angular position.	25
Figure 8 Concept of ToF technology for calculating distance [9]	26
Figure 9 Angle of arrival is calculated, representing the direction from which the received signal was initially emitted [10].	28
Figure 10 Doppler Effect: (a) A static wave source relative to its wave crests. (b) Wave source moving towards right. Assuming we observe a wave source moving towards a direction the wavelength of the source changes relative to its motion [9].	29
Figure 11 Multilateration method: The grey dot location is calculated from the intersection of RSSI signals coming from the three other nodes [11].....	31
Figure 12 A Bluetooth fingerprinting based on the RSS value [12].	32
Figure 13: (a) Example of view sequence (b) Current view to be compared with the view sequence [9].....	34
Figure 14 Three examples of coded targets [9].....	35
Figure 15 Example of different projected reference patterns [9].	35
Figure 16 Thermography of a cat.....	37
Figure 17 Kinect device [14].	38
Figure 18 An example of tracking an object using echolocation [15].	39

Figure 19 An RFID tag.....	41
Figure 20 A passive based RFID object identification [16].....	41
Figure 21 UWB versus other radio communication systems.	43
Figure 22 Passive UWB object localization [9].....	43
Figure 23 Virtua anchor based multilateration [9].....	44
Figure 24 Nine degrees of freedom IMU [20].....	48
Figure 25 Relation of acceleration between velocity and position [21]	48
Figure 26 Inside of an accelerometer	50
Figure 27 Accelerometer made with piezoelectric walls [25].....	52
Figure 28 Capacitance accelerometer	52
Figure 29 (a) basic principle of a gyroscope (b) inside of a capacitance gyroscope	53
Figure 30 Piezoelectric gyroscope.....	53
Figure 31 Hall effect based magnetometer [27].	54
Figure 32 Yaw rotation	56
Figure 33 Pitch rotation	57
Figure 34 Roll rotation.....	57
Figure 35 (a) Arduino Uno board (b)Arduino Nano board	63
Figure 36 (a) Top view of sensor (b)Bottom view of sensor [38]	64
Figure 37 An example of connection between multiple devices with I2C protocol [40]	65
Figure 38 Hookup between MPU9250 and Arduino [38] (a)zoomed in circuit (b) zoomed out circuit (c)circuit with Arduino Nano	66
Figure 39 General diagram of position and orientation estimation	67
Figure 40 Block diagram of AHRS.....	68
Figure 41 Data displayed from serial port in Arduino.	70
Figure 42 Data displayed from serial port in TeraTerm.	70
Figure 43 Data flow	71
Figure 44 UML diagram for assigning the data from .csv into variables.....	71

Figure 45 Block diagram of algorithm	72
Figure 46 (a) XY rail translator (b) Z rail	74
Figure 47 Plots of accelerometer and gyroscope when sensor is stationary.....	75
Figure 48 Plots when moving sensor 60cm at the X axis. Low right the position is displayed.	76
Figure 49 Plots when moving the sensor 40cm to Y axis. Lower right the position is displayed	77
Figure 50 Plots when moving the sensor at 30cm at XY axis. Lower right the position is displayed.....	78
Figure 51 Plots when moving the sensor 30cm at Z axis. Lower right the position is displayed.	79
Figure 52 Plots when moving sensors 30cm at X, Y and Z. Lower right the position plot is displayed with the values.	80
Figure 53 Measurement results when moving sensor at 60cm on X axis	81
Figure 54 Measurement results when moving sensor at 60cm on Y axis	82
Figure 55 Measurement results when moving sensor at 30cm on Z axis.....	83
Figure 56 Measurement results when moving sensor at 30cm on X and Y axis	83
Figure 57 Measurement results when moving sensor at 30cm on X, Y axis and Z axis.....	84

List of Tables

Table 1 Attributes Comparison of linear Position sensors 45

Table 2 Overview of indoor position technologies.....46

Table 3 Overview of accuracies in each movement that was tested. 85

CHAPTER 1

1.1 Introduction

With technology advancing at such a rapid pace, it is no wonder that the developments in science and engineering are being integrated into the medical sector. Any new knowledge of living systems gained through analytical techniques based on engineering sciences contribute to the progress of medicine. This integration has given rise to the interdisciplinary field of biomedical and as a result, created the need to develop more applications at this field.

Prominent breakthroughs in the biomedical field include life-saving and life-changing technology such as artificial organs, bio-sensors, prosthetics, surgical devices, pacemakers, EEGs, regenerative tissue growth, pharmaceutical drugs, kidney dialysis, to name a few. Many biomechanical analyses are also interested in the estimation of the pose (position and orientation) with the use of a sensor [1]. In all the different biomedical applications the ultimate objectives in research and education are to improve the quality of life, reduce the impact of diseases on the everyday life of individuals, and provide an appropriate infrastructure to promote and enhance the interaction of biomedical researchers [2].

The growing demand for low cost, conformal, portable and durable sensors are driven by biomedical applications. The major challenge about this type of applications is the need for economic eco-friendly and small sensors that can be easily implemented out in different environments [3].

In this thesis, we propose a position tracking device able to display a 3D coordinate of its position when it moves that can be embedded in biomedical applications. A position tracking

device usually contains a sensor and it is responsible for detecting the precise position of an object in 3D(three-dimensional) space, this systems often called Indoor Position Systems(IPSs).Sensor record the signal from the real object when it moves or is moved and transmit the received information to the computer [4]. An Indoor Position System (IPS) is a system responsible for providing the location of objects (or people) in the form of coordinates in enclosed environments such as the inside of a building where a Global Positioning System (GPS) cannot operate due to weak signal and interference. Because the commercial IPSs are really expensive we decided to make ours with the lowest cost as possible, easy to implement at any environment and portable using tools that will minimize the development and maximize the efficiency. The proposed solution has been tested at the Electronics lab.

The rest of the thesis is organized as follows. In the first chapter some applicability and user requirements are also presented along with background theory, in the second chapter some related position sensors are presented as well as some other technologies. In the third chapter our sensor is explained, some theory that was used and the software implementation as well as the hardware implementation. In the fourth chapter, the experiments are presented as well as the accuracy and repeatability of the sensor. The fifth chapter, concludes the present thesis, presents some limitations and proposes future improvements.

1.2 Applicability and User requirement

Tracking systems has grown to be one of the most rapidly evolved technological fields over the past decade. Day by day businesses endow massive amounts of money for positioning systems. Present day lifestyle involves location-based applications to aid us in everyday life accomplishments. This development of the current systems is closely tied to the different requirements determined by each application. Consequently, the need for dedicated local infrastructure for addressing requirements set by the application is indubitable. Therefore, it is necessary to list the performance parameters of these kind of systems. Below we present list of applications that require tracking other than the biomedical as we mentioned before.

- Location-based services in indoor environments (e.g. warehouses, train stations etc.)

- Private homes (e.g. ambient assistant living systems for elderly people, medical monitoring etc.)
- Context detection and situational awareness (e.g. car collision, assisted parking etc.)
- Triggered context aware information services (e.g. museums parks etc.)
- Motion capturing (e.g. movies, video games etc.)
- Computer vision (e.g. virtual reality, augmented reality, robotics etc.)

Each field listed has different prerequisite for position detection. It is obvious that location-based services in warehouses should not share the range and accuracy of positioning in biomedical applications. Therefore, an essential factor for creating a tracking system is to know the user requirements. A list of the most important user requirements contains:

- Accuracy (e.g. mm, cm, m etc.)
- Measurement range (e.g. 0-100m.)
- Manufacturing and maintenance costs
- Update rate (on request or periodically e.g. 200Hz, once a week etc.)
- Scalability
- Robustness (in terms of e.g. physical damage, theft etc.)
- Repeatability

The diversity of the technologies used in tracking position systems arises from the importance of each aspect, given the domain and user requirements. For each specific application, the performance parameters should be coordinated with the user prerequisites, in order to decide upon a suitable positioning technology.

1.3 Background

Tracking position sensors for biomedical applications is really important due to the fact that there are humans involved, that's why high accuracy is critical. There are many ways of estimating the pose (position and orientation) of a body segment. Considering the low-cost, portable with good precision a MEMS IMU sensor was used, specifically the MPU9250 by SparkFun (its price is 15 \$). Micro-Electro-Mechanical Systems, or MEMS, is a technology that in its most general form can be defined as miniaturized mechanical and electro-mechanical elements (i.e., devices and structures) that are made using the techniques of microfabrication. The critical physical dimensions of MEMS devices can vary from well below one micron on the lower end of the dimensional spectrum, all the way to several millimeters as shown in figure 1. Likewise, the types of MEMS devices can vary from relatively simple structures having no moving elements, to extremely complex electromechanical systems with multiple moving elements under the control of integrated microelectronics. The one main criterion of MEMS is that there are at least some elements having some sort of mechanical functionality whether or not these elements can move.

While the functional elements of MEMS are miniaturized structures, sensors, actuators, and microelectronics, the most notable (and perhaps most interesting) elements are the microsensors and microactuators. Microsensors and microactuators are appropriately categorized as “transducers”, which are defined as devices that convert energy from one form to another. In the case of microsensors, the device typically converts a measured mechanical signal into an electrical signal [5].

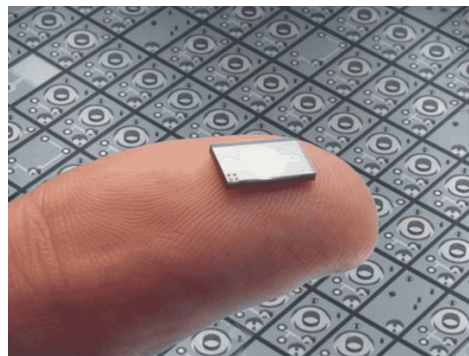


Figure 1 size of a MEMS

CHAPTER 2

2.1 Overview of other position sensors and technologies

Outdoor position systems performance and quality has been increased significantly due to the improvement of worldwide satellite positioning. Nonetheless inside positioning cannot depend on same technologies as outdoor systems. So, it is really important to categorize positioning into outdoors and indoors.

In our application it would be truly simple if the application took place only at an outdoor environment. In that particular case we could use a GNSS (Global Navigation Satellite System) which is basically systems including GPS, GLONASS, Galileo, Beidou [6]. It can be really accurate to achieve our goal which is to track position but the GNSS does not perform efficiently in the inside of structures, as a result of deficient view of the open sky so the signal gets blocked. Therefore, we want to develop a system that work the same in indoors and outdoors environments. Many sensors have used for tracking position but there are not perfect systems yet developed. A system that nowadays evolves really fast is called Inertial Navigation System (INS) and it is based on the sensor we used in this thesis. Below we present some position sensors each having their own strengths and weaknesses.

2.2 Position Sensors

A quick research reveals a very long list of devices that can be used to measure position, but the most widely used solutions in the marketplace fall into 5 main classes. More information can be found at [7].

2.2.1 Potentiometers

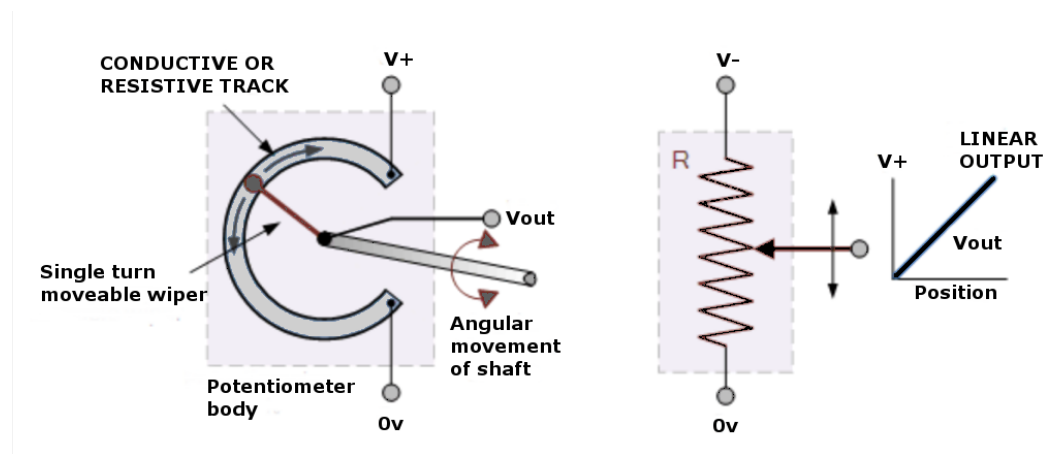


Figure 2 Potentiometer sensor

Potentiometers as shown in figure 2 are a contacting position sensor that use a wiper contact, attached to the moving part, to move along a resistive track. The output will vary depending upon the wiper's position on the track, so resistance is proportional to position. By making the track design curved, pots can be used for rotary as well as linear measurements. They come in a wide range of designs and sizes such as the commonly available round rotational type or the longer and flat linear slider types. When used as a position sensor the moveable object is connected directly to the rotational shaft or slider of the potentiometer [8]. This simple measuring principal means pots have been used for many years in low cost applications with undemanding performance criteria and at their simplest are some of the cheapest position sensors available. They are easy to use and available in a great range of sizes and geometries.

However, they are not recommended for anything other than benign environments, the resistive track is easily eroded by dirt or vibration and accuracy and repeatability are low. If high performance and durability are a concern then potentiometers are not a good fit, although as with most things if enough money is spent on seals, mounting and protection their performance can be improved.

2.2.2 Magnetostrictive position sensors

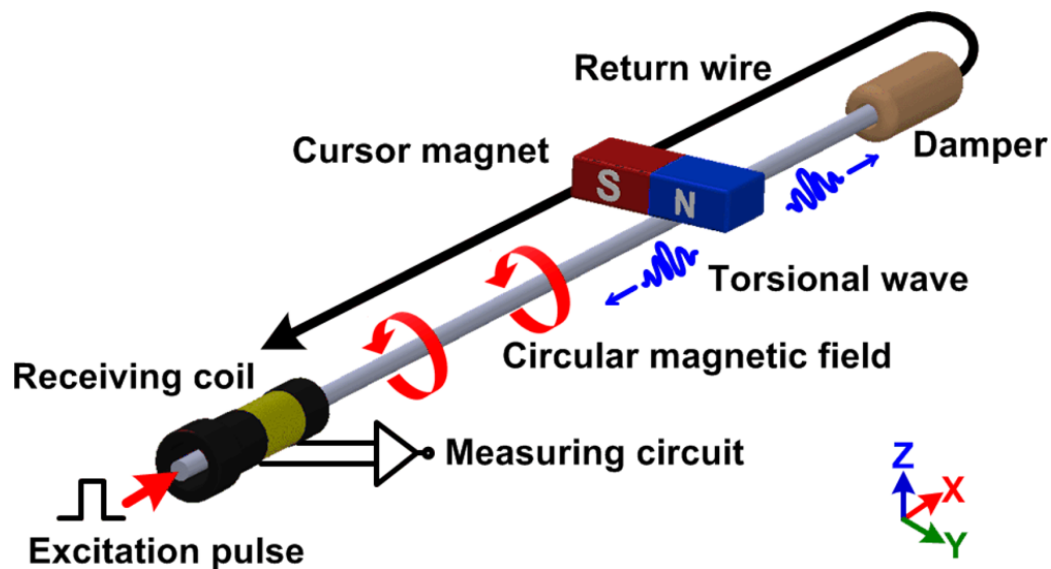


Figure 3 Magnetostrictive sensor

Some ferromagnetic materials (cobalt, nickel, iron) change size or shape when placed in a magnetic field. Magnetostrictive sensors as you can see in figure 3, use this effect. Applying a magnetic field to these materials creates stress, and this can be used to estimate the position of the magnetic field.

A basic magnetostrictive position sensor will attach a magnet to the target object, alongside a waveguide wire attached to the stationary part of the machine. The magnet is used to produce a pulse of magnetic field which will stress the waveguide wire at the point where the

target is. This stress creates a strain pulse which travels at a known rate along the waveguide to the pick up coils, where the timing between pulse and pick up is measured.

This is a technique that works well for linear position rather than rotary position. The waveguide strip and delicate pickup units must be well protected to avoid external stress sources, meaning these sensors are challenging to manufacture and require individual calibration. Consequently, they tend to be higher priced (typically >\$100) and used in high value applications.

Even with the housing, these are not sensors well suited to high vibration or shock applications. The time of flight calculation means there is also a minimum length (roughly <100mm) below which measurement is not possible.

Less obvious is the effect of temperature – extremes of temperature, by causing expansion, can affect the accuracy of magnetostrictive sensors, and data sheets should be read with this in mind.

2.2.3 Encoder – magnetic

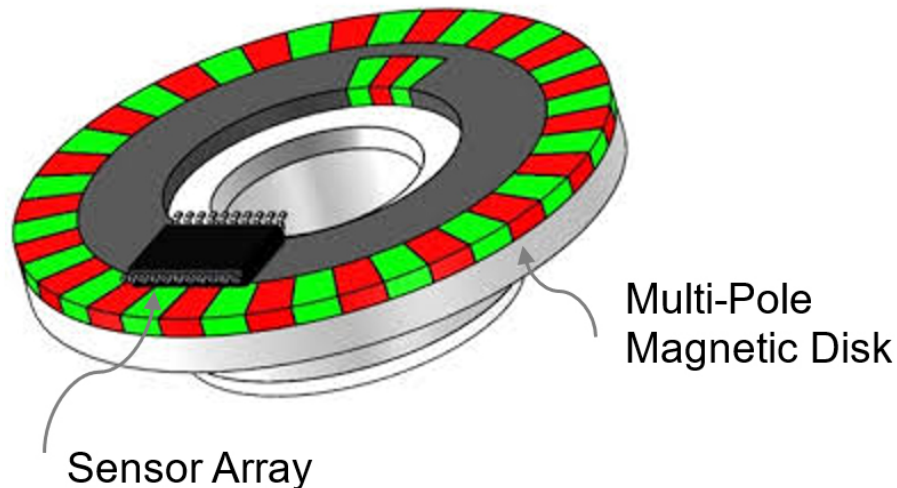


Figure 4 Magnetic encoder

Encoders generally use a scale to measure the position of the target object against a fixed part of the machine. In magnetic encoders, that scale is marked out with a number of magnetic poles – by attaching a sensor to the fixed point and measuring the magnetic poles as they pass the sensor, it's possible to determine the position of the target.

There are a number of sensor options to measure the magnetic poles, but most popular are Hall effect sensors, which vary their voltage in proportion to magnetic field.

These are high volume, low cost sensors and good for applications which don't need linearity below 1%, in other words, applications where accuracy is not a prime concern. Other design considerations to think about:

They work to tight mechanical tolerances which can add some complexity and cost to manufacturing.

There are sizeable temperature effects, so if accuracy is really important, temperature will need to be carefully controlled.

Magnetic encoders can be sensitive to a range of external factors including magnetic hysteresis, external DC/AC fields and the distorting effects of magnetically permeable materials (e.g. steel)

Over time, magnetic encoders can attract metal particles (swarf) which can also affect their accuracy

To sum up, these are high volume sensors suitable for cost sensitive designs where linearity and accuracy is not the first concern and where other factors such as temperature and mechanical positioning, can be well controlled.

2.2.4 Encoders – optical

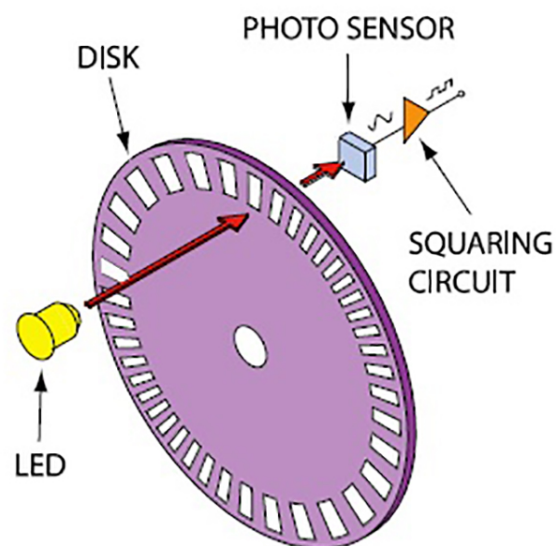


Figure 5 Optical encoder

A popular alternative to magnetic encoders, optical encoders, as the name suggests, use light to identify the position of the target. By shining a light onto a light detector and interrupting that light source with a grid or grating that encodes the position of the target, the light detector will produce a digital output that can be used to find the target position.

As with magnetic encoders, this simple principle covers a lot of different variants: the light can be shone through gratings or reflected back, visible or infra-red light can be used, the encoder disc can be glass or other transparent material.

Optical encoders can be used to determine both linear and rotary position and more expensive products can offer high accuracy and resolution, if used correctly. As a result, they are popular in many industrial automation applications.

In undemanding environments their performance is good, but great care must be taken to mount them accurately because any misalignment has a significant impact on linearity. For this reason, the encoder disc, sensor and processing electronics are often packaged inside a housing including bearings. Seals are usually added for environments where dust, shock or moisture feature. These problems with moisture mean that optical encoders are also a poor fit for products that operate in cold or high humidity environments, condensation can affect reliability.

2.2.5 LVDT/RVDT

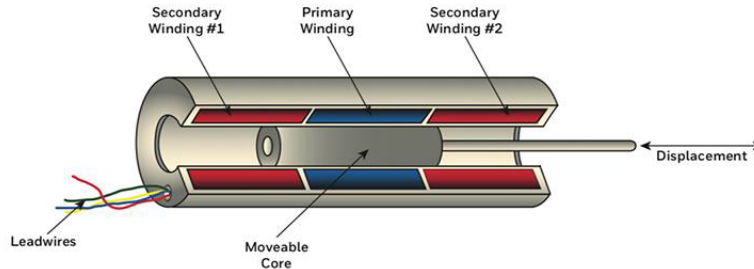


Figure 6 Linear Variable Differential Transformer sensor

Inductive sensors have a good reputation for robustness and accuracy and they are first choice for a range of applications requiring high reliability in challenging environments.

Several types of sensors are based on inductive principles, including simple proximity switches, variable inductance sensors and synchros. These offer a range of performance in respect of cost, resolution and linearity.

Typical examples are LVDTs (Linear Variable Differential Transformer) for linear measurement and RVDTs (Rotary variable Differential Transformer) for rotary. In these sensors, primary coils excite secondary coils in the housing of the sensor. The EMF (Electromotive Force) in the secondary coils will then vary in proportion to their coupling to a moving ferromagnetic core. By using multiple receive coils and calculating the position based on the ratio of signal in each coil confounding factors like temperature can be removed.

Inductive sensors are unaffected by dirt and moisture and as the sensing components can be located well away from sensitive electronics, are well suited to very harsh environments.

They are not without drawbacks; some types of sensor need shielding from stray magnetic fields, for LVDTs/RVDTs the precision windings make them bulky and relatively expensive, limiting their use to higher value applications in areas like aerospace and process industries.

2.2.6 Resonant inductive position sensing

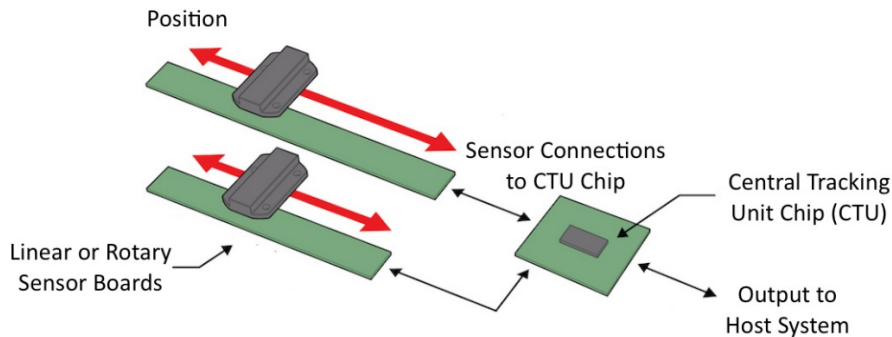


Figure 7 Inductive position sensor for linear and angular position.

A modern evolution of inductive sensors that is gaining traction in many applications, resonant inductive position sensing reduces the drawbacks of bulk and cost by embedding the coils in PCB (Printed Circuit Board). This offers greater precision at a much reduced cost and footprint.

By using an electrical resonator in the target, the system can use a pulse echo approach – the resonator is inductively powered by an excitation circuit, then the power is removed and the system detects the response of the position sensing coils to the target. This removes cross coupling errors from the system and produces much better signal and higher tolerance for misalignment, free from any calibration.

Overall, resonant inductive position sensing is very well suited for any application which requires high performance – it can be engineered to very high levels of linearity and offers high sample rates. It is even more robust than traditional inductive position sensing approaches, requiring little protection from dirt, moisture, vibration or shock.

2.3 Other Related Technologies to Tracking Position

In this chapter we present some other technologies that does not contain the previous position sensors. This kind of systems are widely used for localization and tracking applications. Before we explain these systems, we need to clarify some terms.

2.3.1 The Basic Position Measuring Principles

The basic position measuring principles are some common techniques for angular and distance observations which form the basic methods that will be explained at section 2.3.2

Time of Arrival (ToA) / Time of Flight (ToF)

Time of Arrival (ToA), sometimes called Time of Flight (ToF), is the travel time of a radio signal from a single transmitter to a remote single receiver (Figure 8). The distance between the two can be derived by the multiplication of the signal travel time by the wave speed. Since the wave speed relies upon the properties of the propagation medium, information of the intermediate material (e.g. air, concrete etc.) is required. Synchronization of transmitter and collector clocks is important, as even one nanosecond blunder in synchronization translates into a distance error of 30 cm if radio frequency signals are utilized.

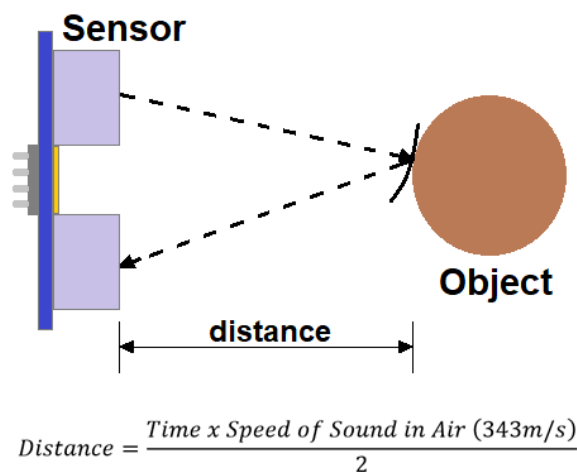


Figure 8 Concept of ToF technology for calculating distance [9]

Time Difference of Arrival (TDoA)

TDoA, as the name implies, follows the same tactic as ToA with the variance that in TDoA the receiver does not need to know the absolute time at which a pulse was transmitted, just the time difference of arrival from the synchronized transmitters. With that in mind, constant time offset caused by a clock bias is subtracted from ToA measurements. With two emitters at known locations, a receiver can be located onto a hyperboloid. A receiver's location can be determined in 3D from four emitters by intersection of three hyperboloids. With this methodology, very precise synchronization of all emitters is a precondition. For GNSS positioning TDoA is a useful approach, because the drift of a low-cost receiver's clock can be eliminated while the satellites are precisely synchronized by 'GNSS time'. Alternatively, a portable emitter can be located from numerous receivers. In this arrangement, the static nodes-receivers are attempting to decide the location of the portable station.

Round Trip Time (RTT) / Round-trip Time-of-Flight (RToF) / Two Way Ranging (TWR)

RTT, otherwise Two-Way Ranging (TWR), is the time required for a signal pulse to make a trip from a specific source to a specific destination and back again. RTT eliminates the need of time synchronization between the transmitter and the receiver, permitting its use in uncoordinated mesh-like networks. As a disadvantage, critical latencies may occur because the range estimations to multiple devices should be completed consecutively for applications where devices move rapidly. However, this method has the benefit of low complexity and cost.

Phase of Arrival (PoA) / Phase Difference (PD)

PoA utilizes the received carrier phase to decide the separation between two devices. Keeping in mind the end goal to mitigate phase wrapping, the received signal phase is assessed on multiple frequencies. The distance is then determined by the rate of phase change.

Near-Field Electromagnetic Ranging (NFER)

NFER refers to any radio technology utilizing near-field properties of radio waves. It employs transmitter tags and one or more receiving units. The phase of an electro-magnetic field changes according to the distance around an antenna. Depending on the choice of frequency, NFER has potential estimations in the precision scope of 30 cm to 1 m and operating distances up to 300 m.

Angle of Arrival (AoA)/Angulation / Triangulation / Direction-based Positioning

Angle of arrival (AoA) is a method for determining the direction of propagation of a radio-frequency wave incident, on a direction sensitive antenna array (Figure 9). AoA determines the direction by measuring the Time Difference of Arrival (TDOA) at individual elements of the array. By measuring these delays, the AoA can be calculated.

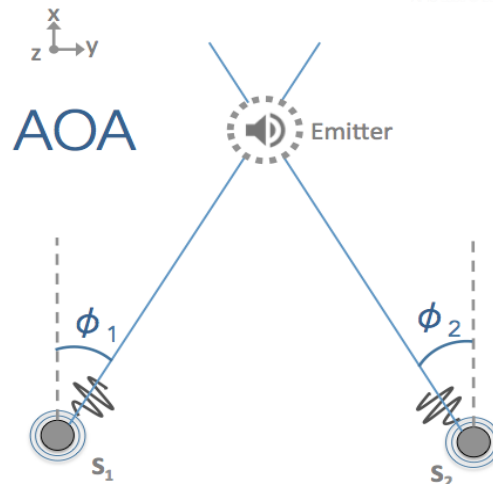


Figure 9 Angle of arrival is calculated, representing the direction from which the received signal was initially emitted [10].

Doppler Ranging

The Doppler ranging method uses the Doppler Effect to produce velocity data about objects at a distance. It does this by bouncing a microwave signal off a desired target and analyzing how the object's motion has altered the frequency of the received signal. Given a known

starting position and different Doppler frequency observations, the displacements of a mobile device can be resolved through the measured Doppler frequency shifts (Figure 10).

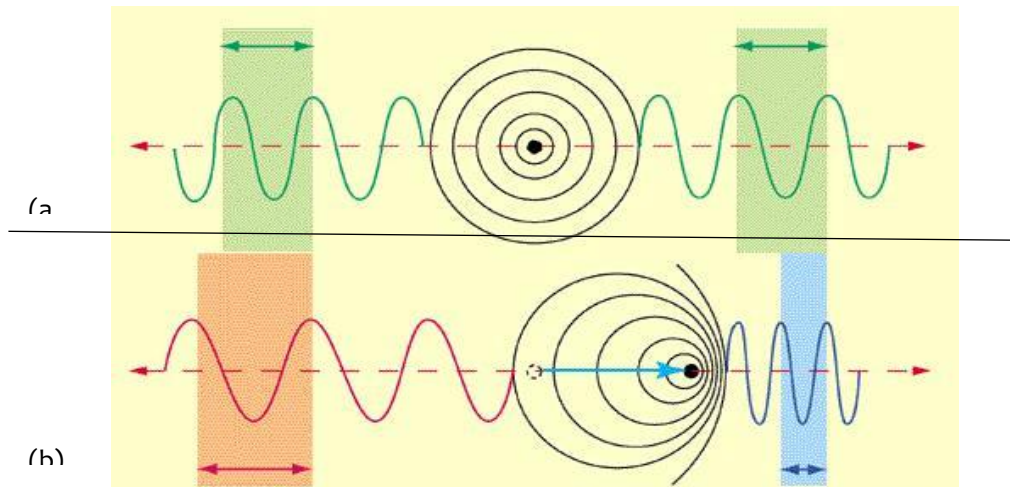


Figure 10 Doppler Effect: (a) A static wave source relative to its wave crests. (b) Wave source moving towards right. Assuming we observe a wave source moving towards a direction the wavelength of the source changes relative to its motion [9].

Received Signal Strength Indicator (RSSI)

In this method, as the name indicates, signal attenuation is used to provide distance estimation based on how far a beacon is from the signal source. By sampling the received signal strength values of source over a time period and calculating its average we are able to produce an RSSI weight mapping of a certain area-volume. RSSI values are measured in decibels, because they are specified as power measurements. Given a signal source, RSSI range circles are formed in relation to the source based on the integrated signal attenuation model.

2.3.2 Positioning Methods

Following the basic measuring principles used in positioning, we introduce the most common positioning methods used in the field. The determination of position of an object is given through measurements of proximity, distance and angular information.

Cell of Origin (CoO) / Proximity Detection / Connectivity Based Positioning

CoO method determines the position of a target by its existence in a particular area. The location of the base station is ascertained and the location of the caller is considered to be where the strongest signal is received. CoO is not a very precise locator and its accuracy depends on the number of base stations in the search area and the signal range. CoO is a simple positioning method used for applications with low requirements in terms of accuracy. Examples are sensors detecting physical contact and mobile wireless positioning systems.

Centroid Determination

Given a set of multiple beacon positions (e.g. Wi-Fi transmitters), the centroid beacon is to be located. The most common method of centroid determination is through RSSI values. The position of the centroid beacon can be determined by the weights in form of RSSI values measured by the centroid beacon. Knowledge of the positions of each beacon within the detection area is a requirement of this technique.

Lateration / Trilateration / Multilateration

Each of these terms contains the process of determining absolute or relative locations of points by measurement of distances to nearby nodes (Figure 11). The most common techniques used for distance measuring are the RSSI, ToA, TDoA and RTT.

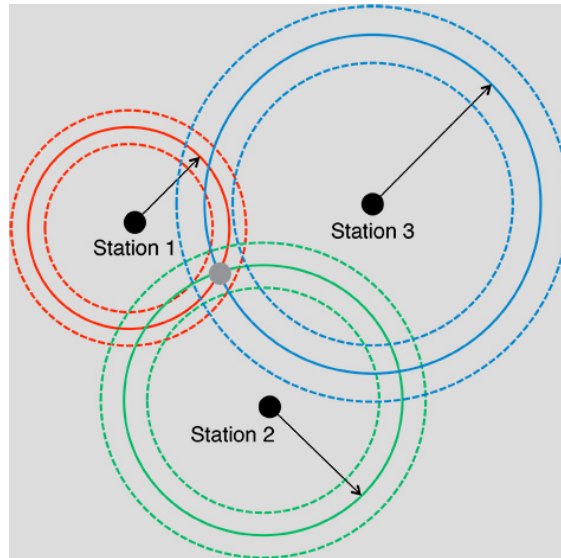


Figure 11 Multilateration method: The grey dot location is calculated from the intersection of RSSI signals coming from the three other nodes [11].

Fingerprinting (FP) / Scene Analysis / Pattern Matching

Fingerprinting is a procedure that maps data (such as RSSI values, images or audio signals) that are uniquely identified, just as human fingerprints uniquely identify people for practical purposes. The fingerprinting algorithm has two phases: the off-line calibration stage and the on-line measurement stage. In the first stage, a database with all the unique fingerprints is created, mapping the scene. In the second stage, the fingerprint measured by the online phase is compared with the database created in the first stage and the best fit is computed. Assuming we scatter multiple Wi-Fi or Bluetooth beacons across a building or room, we create a database with the measured RSSI values taken in each room of the building as shown in figure 12 .In the online phase, the current RSSI value is compared with the values gathered and the best matching/fit reveals the coordinates.

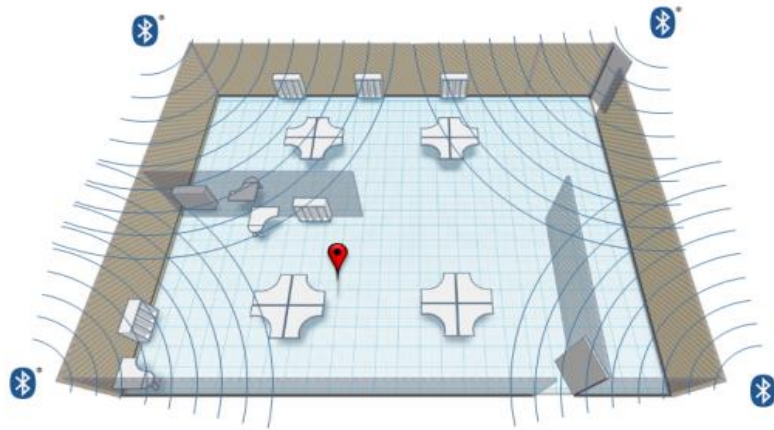


Figure 12 A Bluetooth fingerprinting based on the RSS value [12].

Dead reckoning (DR)

In navigation, dead reckoning (DR) is the process of estimating usually a pedestrian trajectory and position by using a previously determined or fixed position and advancing that position based upon known or estimated speeds or accelerations over time. A system of inertial navigation uses DR to estimate current position by measuring the speed over an elapsed time in relation to its starting position. The sensor types used in DR are accelerometers and gyroscopes.

2.3.3 Technologies

In this chapter we will present some technologies that are used in Indoor Positioning Systems, more details at [13].

2.3.3.1 Cameras

Optical indoor positioning utilizes cameras as the main type of sensor. A wide variety of applications with different requirements of accuracy can be produced using cameras. The main reason behind this is the advancement in the technology of detectors (e.g. CCDs) and the decrease in size of actuators (e.g. lasers). However, camera's fundamental application zone is in the sub-mm domain. This means that cameras are typically used in applications

requiring millimetric or sub-millimetric accuracy. With the advancement of image processing algorithms and faster data transmission rates, optical methods have become a great technique of positioning.

There are two main types of optical indoor positioning systems involving cameras. In the first method, a mobile camera mounted on the user is to be located by reference images captured by it. Comparison between the current image and the pre-gathered reference images reveals the camera location. In the second method, static cameras capture the moving target and turn the 2D observations of the CCD into 3D coordinates. Rotation measurements are based on the Angle of Arrival (AoA) technique. When more than one camera is used, depth information can be calculated by stereo vision algorithms. However, depth acquired from monocular images can be obtained by sequential observations of the scene, using a synthetic stereo vision approach.

The transformation from the CCD image into the actual object location cannot be resolved without additional information regarding the distance. Moreover, the baseline between the cameras must be known beforehand. Laser scanners and range imaging sensors can be used in tandem with cameras for obtaining more accurate distance measurements.

A rough categorization of optical positioning systems can be performed based on how the reference information is obtained, as described next.

Referencing from 3D Building Models

In this category, camera images containing specific objects are compared to interior design databases. From this comparison, location and angle can be detected based on the geometric properties of fixed objects like windows and doors. The main feature of these kinds of methods is that there is no necessity for local infrastructure, because real sensor beacons are substituted by digitally created referencing points through images. In this way, the extra cost imposed by scaling coverage, is eliminated as well.

Reference from Images

This class of positioning methods, also mentioned in the literature as view-based approaches, consists of two stages. In the first stage, sequences of images are gathered along multiple paths inside a building. In the second stage, the current view of a mobile camera is compared to the previously captured view sequences as showed in Figure 13. As a drawback, an external reference source must be utilized sporadically to regulate accumulated deviations.



Figure 13: (a) Example of view sequence (b) Current view to be compared with the view sequence [9].

Reference from Deployed Coded Targets

Another commonly used method of optical positioning is the deployment of unique markers as shown in Figure 14. These markers are scattered throughout the coverage area and uniquely stamp the desired regions. Coded markers can be placed in different locations (e.g. floor, walls) depending on the way they are being recognized by the sensor. Compared to systems relying entirely on natural features of CCD images, coded targets are more reliable under conditions of varying illumination. As a result, the level of accuracy from the reference points is higher, making it suitable for positioning systems demanding higher accuracy requirements. Last but not least, they simplify the process of image detection thanks to the use of well-defined geometrical shapes and coloring.

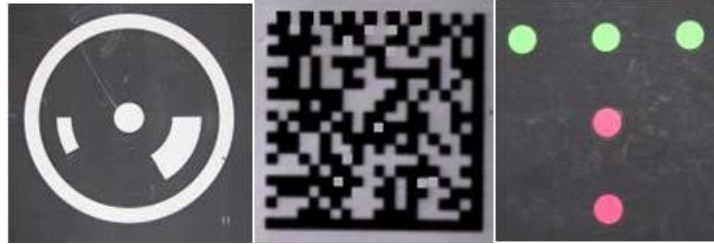


Figure 14 Three examples of coded targets [9].

Reference from projected targets

If mounting of reference markers is not a possible or desirable solution, one can turn to a different approach by projecting reference points or patterns in the desired area from complementary devices such as LEDs or projectors (Figure 2.11). A common way is to project infrared light in order to attain unobtrusiveness to the user, because the infrared light cannot be perceived by the human eyes. Location of the user is calculated by differentiations in color or shape of the pattern projected. This method eliminates the cost of physical reference targets.

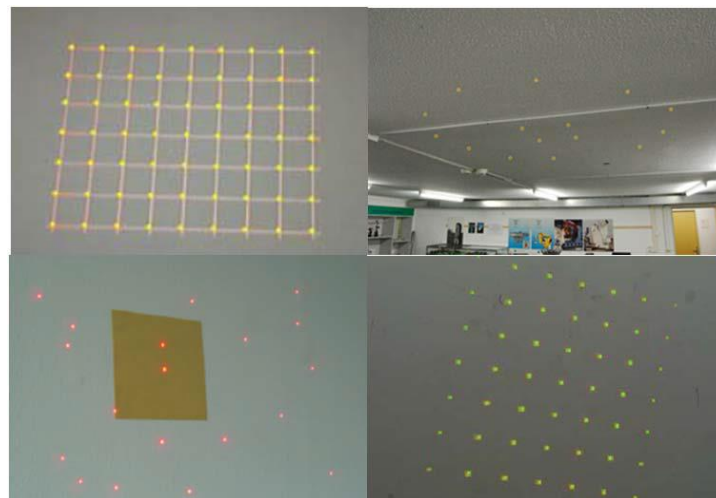


Figure 15 Example of different projected reference patterns [9].

Systems without Reference

In this category fall all systems deploying static cameras with high frame rates for position detection. Real-time tracking is accomplished by observing the differences in images of subsequent frames. This method requires the placement of orientated static cameras on fixed, known, locations.

2.3.3.2 Infrared

Infrared radiation has been used extensively in positioning systems due to fact that it is invisible to the human eye compared to visible light. There are three major categories that utilize IR radiation to perform position detection: active beacons, IR imaging with natural radiation and IR imaging with artificial light sources.

Active Beacons

The architecture of systems utilizing active beacons consists of placing infrared receivers throughout the coverage area on fixed, known locations. A mobile unit or “active beacon” mounted with an IR emitter is then located based on which receiver picks up its signal. Several IR emitters or beacons with different IR frequencies can be located simultaneously. Angular information can be obtained by installing optical polarizing filters on the IR receivers. Active Beacon positioning has a low accuracy level and is used for room-to-room localization.

Position detection with Natural Infrared Radiation

Natural Infrared Imaging, also known as infrared thermography, measures the surface temperature of an object through its heat emission. Positioning systems with IR sensors operating between 8 μm to 15 μm - long infrared spectrum - are also referred as passive infrared systems. Thermal infrared radiation can be used to track people or objects through their temperature, as shown in figure 16, without the need of external components. However, strong infrared radiations from sources like the sun or bright ceiling lights can deteriorate the detection accuracy. Thermal cameras, pyro-electric infrared sensors and thermocouples are the most common detectors for performing passive localization.



Figure 16 Thermography of a cat

Position detection with Artificial Infrared Light

Optical IR positioning with artificial IR light imaging involves the use of active IR light sources with IR-sensitive cameras. This method is commonly used as an alternative to visible light optical positioning systems. Implementations using IR cameras are either based on active infrared LEDs or on retro-reflective targets. In the first approach, the target is mounted with one or several active infrared LEDs and its position is detected by a CCD IR camera. In the second approach, an external IR source illuminates the target and then the reflected light is gathered by the CCD.

Microsoft's well-known "Kinect" device utilizes IR technology as shown in figure 17. Kinect employs an IR projector capable of covering a room-size space with a predetermined pattern of infrared dots, an IR sensor, which is placed at a given distance relative to the IR projector, capturing the IR dots and an RGB camera. The monochrome IR sensor calculates the distance of the objects captured by its CCD, by subtracting the observed object distance relative to the expected, unobstructed pattern view. People can be tracked simultaneously up to a distance of 3.5 m at a frame rate of 30 Hz. An accuracy of 1 cm at 2 m distance has been reported.



Figure 17 Kinect device [14].

2.3.3.3 Sound



Animals and humans can determine their position and orientation in dark spaces by listening to sounds of the environment they are into. In science, this is referred to as sound localization. Sound localization is based on the propagation of sound waves in space. Positioning systems utilizing sound waves locate mobile nodes by determining absolute or relative locations of points by measurement of distances to nearby nodes. Static nodes are mounted on walls, ceilings or even on the floor. There are two main types of sound positioning systems, active and passive device localization. In the first type, the mobile node is a sound emitter and its location is calculated from the fixed - already known - positions of static nodes. Alternatively, passive device localization consists of multiple static sound emitters and a passive node listener. Ultrasound is more commonly used in these systems compared to audible sound for attaining unobtrusiveness to the users. However, audible sound systems can be easily implemented through sound cards of standard devices.

Ultrasound

Ultrasounds are high frequency sound waves which are non-audible to the human ear. Distance calculation is performed through Time of Arrival (ToA) measurements. However, the operating range of ultrasound emitters is less than ten meters as a result of the sound wave

intensity decay in the transmission channel. In the ToA method, synchronization of the mobile node with the static nodes is required. To overcome this problem, most ultrasound positioning systems utilize the Time Difference of Arrival (TDoA) method to enable ad-hoc localization. Mobile nodes broadcast a radio frequency signal in tandem with the ultrasound pulse to inform close-by static nodes of their presence.

Echolocation

In enclosed rooms, not only the direct sound from a sound source is arriving at the listener's ears, but also sound which has been reflected at the walls. Bats, among many other animals, use this technique called bio-sonar to determine their position and locate objects within their perimeter as shown in figure 18. Similar solutions have been created for eliminating the need for beacons and tags in sound positioning systems. In order to determine the time periods where the direct sound prevails the secondary, object-bounced, sound, the auditory system analyzes loudness changes in different critical bands and also the stability of the perceived direction.

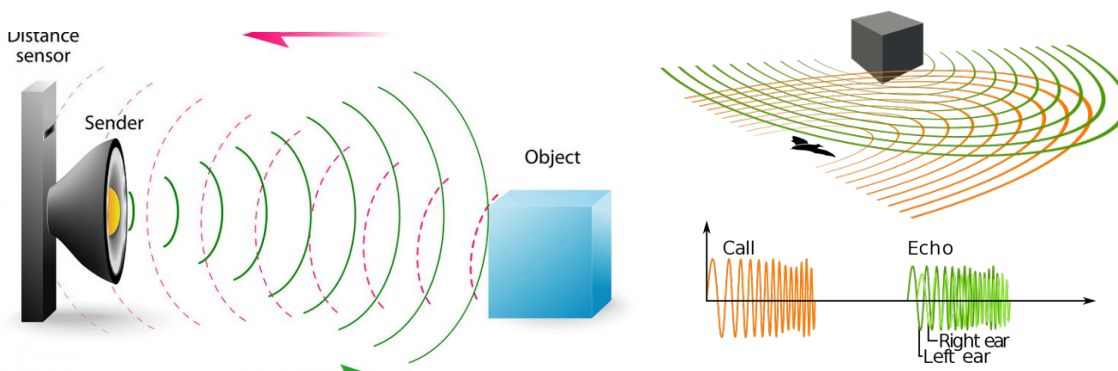


Figure 18 An example of tracking an object using echolocation [15].

2.3.3.4 RFID



RFID is an acronym for “radio-frequency identification” and refers to a small device that contains of a tiny chip and an antenna. This small device also called RFID reader, scans the surroundings using electromagnetic fields for the RFID tags as shown in figure 19, these tags are separated into active and passive. Data can be transmitted from the RFID tags to the reader via radio waves. Each RFID tag has its own unique ID, typically a serial code, and other information regarding its identity. RFID tags are used in many industries (Figure 20), since they can be easily attached on objects, such as clothing and pharmaceuticals, or even implanted on livestock (e.g. cattle).

Regarding positioning systems, the principles used are the CoO, RSSI and FP. The CoO method is frequently used because of its simplicity. The presence of an object, which has an RFID tag attached on, is reported back to the reader. However, the accuracy of such a system depends on the number of RFID tags used and, of course, the reading range. The RSSI method uses the range estimations between the reader and the spread tags in order to apply multilateration techniques. The Fingerprinting (FP) method on RFID positioning is applied by signal mapping of the RFID reader or the active tags. Last but not least, systems operating with the ToA, PoA and AoA methods have been introduced but have been proven difficult to be utilized due to precise time synchronization required by these methods.

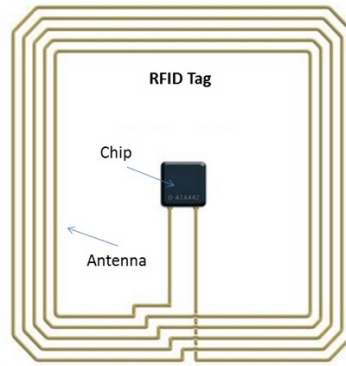


Figure 19 An RFID tag.

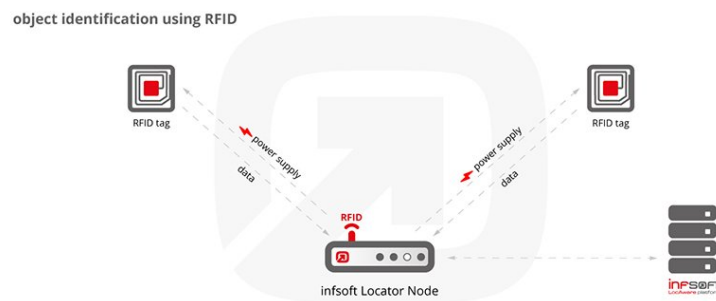


Figure 20 A passive based RFID object identification [16].

Active RFID

Active RFID systems use battery-powered RFID tags that continuously broadcast their own signal. Active RFID tags are commonly used as “beacons” to accurately track the real-time location of objects. Active tags provide a much longer reading range (above 30 meters) than passive tags, but they are also much more expensive and heavier. Positioning systems utilizing active RFID tags are based on the Fingerprinting technique with RSSI values.

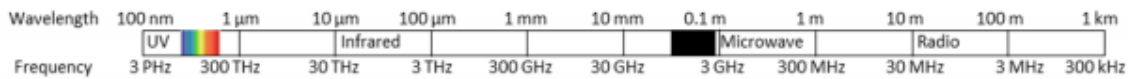
Passive RFID

Passive RFID systems use tags with no internal power source and therefore do not require batteries to operate. The power required to function is transmitted from the RFID reader through radio waves (i.e. inductive coupling). When a passive tag is stimulated from the RFID reader, it reports its unique ID. Positioning systems based on passive tags consist of several

tags scattered in different locations (mesh-like or grid-like). Each tag performs the role of a waypoint and their locations are stored in a database.

Passive tags are suitable for positioning purposes due to their small size, low price, cost-free installation and low maintenance needs, since no internal power source, such as batteries, is required to operate. However, a dense arrangement of tags is usually required because their detection range is often less than two meters.

2.3.3.5 Ultra-Wideband



Ultra-Wideband (UWB, also known as, ultra-band) is a radio technology. UWB transmits information spread over a wide bandwidth (>500 MHz) for short-ranges (i.e. less than 100 meters) with a very low energy level as shown in figure 21. Indoor positioning utilizing UWB is a commonly used approach because of its multipath resistance and penetrability of building materials. UWB transmits in a manner that it does not interfere with conventional narrowband and carrier-wave transmission systems in the same frequency band.

The classic UWB positioning system consists of a radio wave transmitter and several receivers, which identify the broadcasted and scattered waves. A radio wave is perceived to be UWB if its bandwidth is larger than 500 MHz or 20% of the fractional bandwidth.

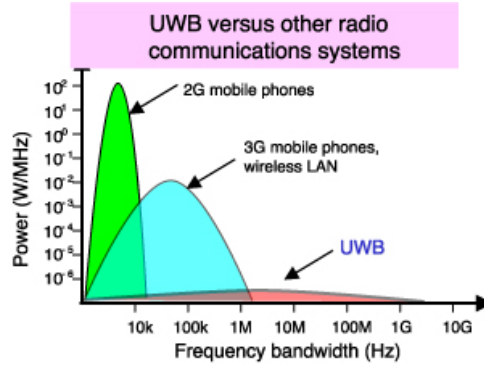


Figure 21 UWB versus other radio communication systems.

Passive UWB localization

In passive UWB localization systems, the target's position is calculated through signal reflection (Radar principle). The typical setup consists of omnidirectional antenna emitters and listeners with known locations. Position and distance measurements of the moving target can be determined by ToA, TDoA and other range-based algorithms. In more detail as shown in figure 22, the direct (from emitters) and the reflected wave signals (from the moving person) are subtracted in time. Thus, their time difference reveals the distance traveled, given that the emitters and receiver antennas locations are known.

Its main advantage is that there is no need for active or passive tag attachments. Thus, there is no restriction in the user's movement caused by wearable hardware.

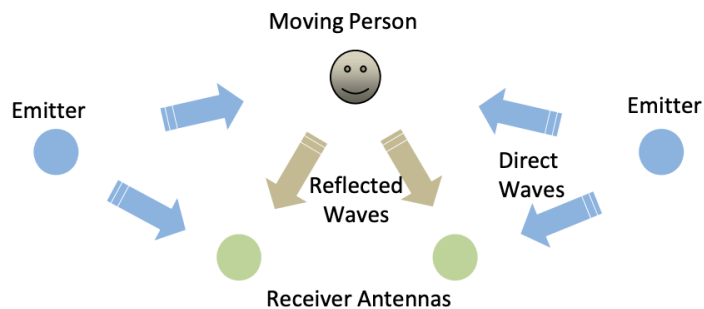


Figure 22 Passive UWB object localization [9].

UWB Virtual Anchors

When the floor-plan information is a-priori known, the position of the receiver is estimated from the signal reflections in the room walls and the direct signal path. This means that we can acquire position information from even a single UWB transmitter. The distances derived from the delay of signal reflections from walls (virtual anchors) can be used for multilateration.

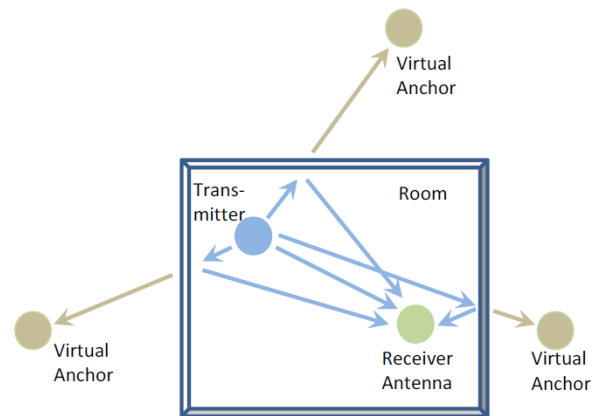


Figure 23 Virtual anchor based multilateration [9].

2.4 Comparison

In this paragraph we will display a table that compares the position sensors that we presented, more information at [17], as well as a table with the other technologies.

Table 1 Attributes Comparison of linear Position sensors

Characteristics	Potentiometer	LVDT	Magnetostrictive	Optical Encoders	Magnetic Encoders	Resonant Inductive
Range	2.5-500mm	2.5-500mm	0.15-3m	0.15-1.5m	0.15-3m	25-200mm
Accuracy	Moderate	Very Good	Excellent	Excellent	Very Good	Very Good
Repeatability	Fair	Excellent	Excellent	Very Good	Very Good	Excellent
Linearity	Moderate	Good	Very Good	Very Good	Very Good	Good
Cost	Low	Moderate	High	Moderate	Moderate	Low
Applicability	Robotics	Automation	Automation	Car Industry	Car Industry	Remote Monitoring

Table 2 Overview of indoor position technologies

Technology	Typical Measuring Principle	Typical Application	Disadvantages
Cameras	AoA	Robot navigation	High cost, more complexity
Infrared	Thermal Imaging, active beacons	People tracking	Expensive system hardware and maintenance cost
Sound	ToA, TDoA	Collision detection	Measures distance, more accurate more receivers are needed so higher cost, affected by temperature
RFID	FP, Proximity detection	Security	Large number of RFID tags needed so more complexity and higher cost
Ultra-Wideband	ToA	Automation, Robotics	Many anchors are needed so higher cost and higher complexity

CHAPTER 3

3.1 The Proposed Sensor

The sensor that we used as previously mentioned was the MEMS (micro-electronic-mechanic-system) IMU (Inertial Measurement Unit) in order to overcome the high cost and inaccuracies of the other technologies. An IMU sensor offers a lot of things such as high update rate, low cost, low power and high accuracy to name a few. Nowadays IMU sensors have entered our lives, you can find them everywhere, in AR(augmented reality) and VR(virtual reality) systems where they are used for tracking the users head movement, you can also find it with an implemented GPS(Global Positioning System) for orientation purposes and finally there is an IMU inside our cellphones for motion tracking purposes. To sum up, IMUs are strong demanded lately one significant trend driving this growth is increasing demand for MEMS (microelectromechanical system) devices, which are generally 20 micrometers to 1mm in size. Other than the physical size, the increasing demand by smartphones is driving down the cost of MEMS (microelectromechanical system) IMU (inertial measurement unit) [18].

3.2 IMU

The Inertial Measurement Unit is an electronic device that measures and reports a body's specific force, angular rate and surrounding magnetic field, using combination of accelerometers, gyroscopes and magnetometers [19]. They are self-contained systems that measure linear and angular motion of an object. Measurements are summed over a time period to determine the instantaneous position, velocity, orientation and direction of movements. IMUs usually measure nine degrees of freedom. This includes the measurement

of linear motion over three perpendicular axes (surge, heave and sway), as well as rotational movement about three perpendicular axes (roll, pitch and yaw) and magnet field strength over the same three axes of rotation. This yields nine independent measurements that together define the movement of an object. The IMU possesses a triaxial accelerometer, or otherwise uses multiple accelerometers that are aligned across perpendicular axes. Additionally, IMU contains multi-axis gyros to provide measurements in three orthogonal directions. And lastly it often contains a 3-axis magnetometer. IMU is used for plenty of applications which one of them is pose estimation(position and orientation).Our approach is based on the simple mathematical equation as shown in figure 25, acceleration is closely related to position because as it is well known from simple physics if we integrate acceleration once we get velocity and if we integrate velocity we obtain position. In figure 24 we can see the 9 Degrees of Freedom of an IMU sensor.

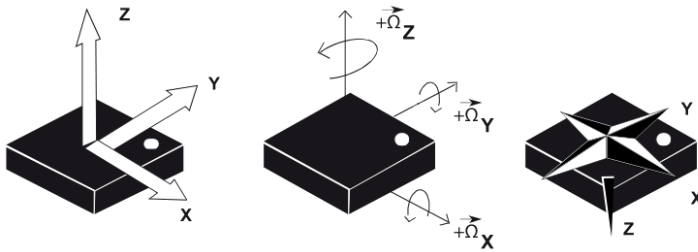


Figure 24 Nine degrees of freedom IMU [20].

$$v = \int a dt$$

$$x = \int v dt$$

Figure 25 Relation of acceleration between velocity and position [21].

3.2.1 Accelerometer

A simple accelerometer contains of a proof mass attached to strings that is inside a case as shown in figure 26. This mass can move inside the case along the accelerometer's sensitive

axis. If an accelerating force is applied to case the mass will tend to remain its previous velocity, so the case will keep moving with respect to the mass, compressing one spring and stretching the other. The forces that the spring transmits changes. Therefore, the case will move due to the asymmetric forces with respect to the mass until the acceleration of the mass exerted by the springs matches the acceleration of the case due to the externally applied force. The resultant position of the mass with respect to the case is proportional to the applied acceleration. By measuring this with a pickoff, we obtain acceleration.

The mass also senses the gravitational acceleration. This acts on the mass directly, not by the springs and applies an acceleration on the accelerometer, so there is no relative motion of the mass with respect to the case. So, accelerometers sense only the nongravitational acceleration, known as specific force. Specific force is the difference between the true acceleration and the acceleration due to gravity. Therefore, specific force contains sensor's acceleration and earth's gravity. Also, the accelerometer measures the specific force with respect to inertial space, which does not accelerate or rotate with respect to the rest of the universe. An IMU computes the specific force vector, f_{ib}^b , where the subscript ib denotes the measurement of the origin of an IMU body frame b , with respect to an inertial frame, i , and the superscript b denotes that the components of the vector are resolved along the axes of the IMU body frame, which normally coincide with the sensitive axes of the constituent sensors. The specific force can be expressed as the inertially referenced acceleration, a_{ib}^b , and the gravitational acceleration, γ_{ib}^b , using the equation

$$f_{ib}^b = a_{ib}^b - \gamma_{ib}^b$$

However, it is more convenient to express the specific force in an Earth reference acceleration a_{eb}^b . So,

$$f_{ib}^b = a_{eb}^b - g_b^b$$

Where g_b^b is the acceleration due to gravity [22] [23].

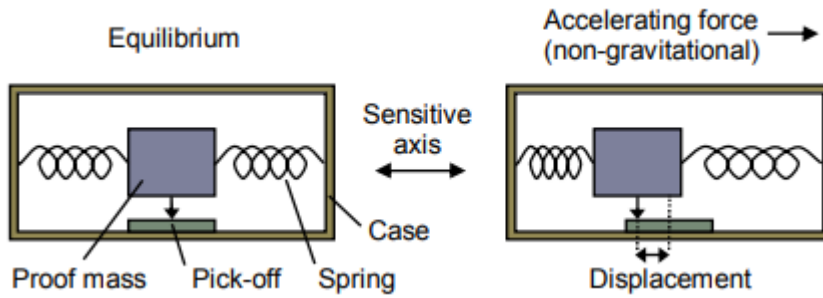


Figure 26 Inside of an accelerometer

There are many ways that an accelerometer works two of them are the capacitance and the piezoelectric effect. The piezoelectric effect uses microscopic crystal structures that become stressed due to accelerative forces. As shown in figure 27 there is a box made of piezoelectric crystals with three pair of sides (each pair represent an axis), whenever the box is tilted ball is forced to move in the direction of the inclination due to gravity. The ball collide to a wall creating piezoelectric currents. Depending on the current, the direction of inclination and the magnitude is determined. The capacitance accelerometer measures the change in capacitance. As shown in figure 28 there is a mass attached to strings that is moving along fixed plates. If an acceleration force moves the mass the capacitance will change and the accelerometer will translate that capacitance to voltage for interpretation. Specifically, the acceleration of the proof mass can be calculated [24].

$$C_1 = e_A \frac{1}{x_1} = e_A \frac{1}{d + x} = C_0 - \Delta C$$

$$C_2 = e_A \frac{1}{x_2} = e_A \frac{1}{d - x} = C_0 + \Delta C$$

So,

$$C_2 - C_1 = 2\Delta C = 2e_A \frac{x}{d^2 - x^2}$$

Measuring ΔC , one finds the displacement x by solving the nonlinear algebraic equation:

$$\Delta C x^2 + e_A x - \Delta C d^2 = 0$$

We get,

$$x \gg \frac{d^2}{e_A} \Delta C = d \frac{\Delta C}{C_0}$$

It is true that,

$$(V_x + V_0)C_1 + (V_x - V_0)C_2 = 0$$

Therefore, we get voltage output V_x

$$V_x = V_0 \frac{C_2 - C_1}{C_2 + C_1} = \frac{x}{d} V_0$$

And finally, we get the acceleration a

$$a = \frac{k_s}{m} x = \frac{k_s d}{m V_0} V_x$$

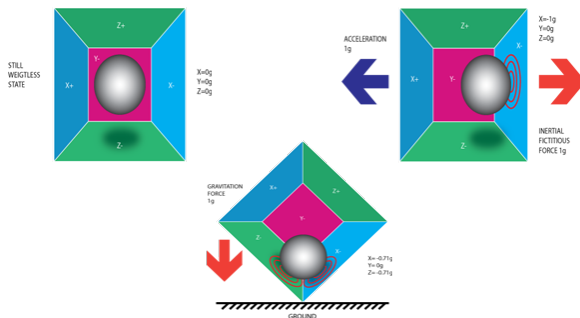


Figure 27 Accelerometer made with piezoelectric walls [25]

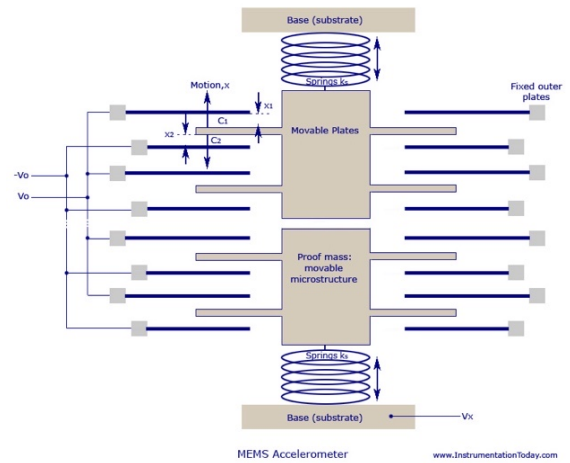


Figure 28 Capacitance accelerometer

3.2.2 Gyroscope

Gyroscopes measure angular velocity with respect to the inertial frame using an effect called Coriolis acceleration. As shown in figure 29 when a mass is moving in a particular direction with a particular velocity and an external angular rate will be applied then a force will occur that will cause perpendicular displacement of the mass. This process will cause a change of capacitance which will be translated in an angular rate. The inside of a gyroscope is shown at the figure 29(b), it contains of mass that is moving and when an external angular rate is applied it will cause the flexible part of the mass to move and create the perpendicular displacement.

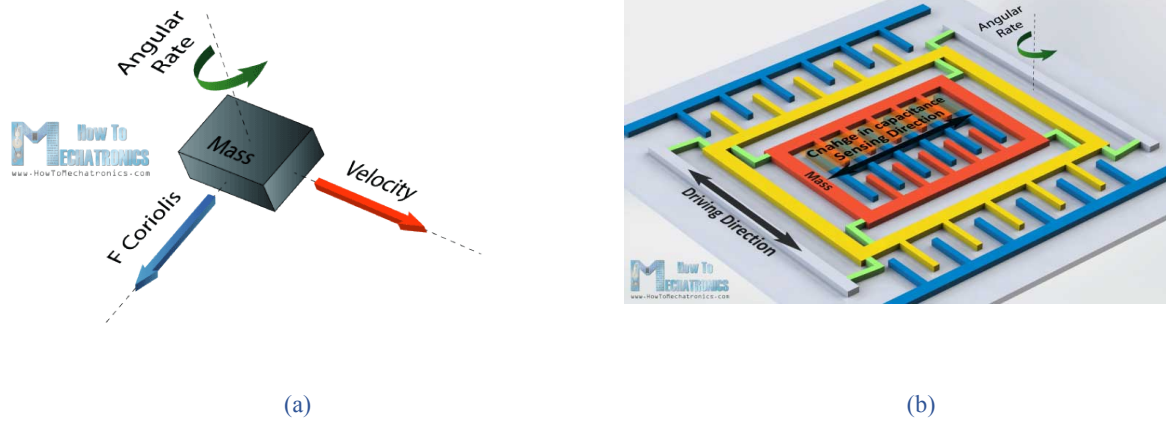


Figure 29 (a) basic principle of a gyroscope (b) inside of a capacitance gyroscope

There are also gyroscopes that work with the same principle but they exploit the piezoelectric effect. The mass is now inside of box as shown in the figure 30 that is made of piezoelectric crystals. When the box is tilted the crystals will experience a force in the direction of inclination. This is caused as a result of the inertia of the moving mass. Therefore, the crystals will produce a current caused by the piezoelectric effect. This current will be converted in an angular rate.

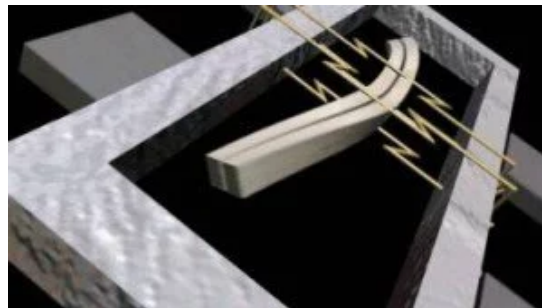


Figure 30 Piezoelectric gyroscope

3.2.3 Magnetometer

Magnetometers measure the earth's magnetic field using the Hall effect. As shown in the figure 31 there is a semiconductor plate that flows continuous current through it. When the circuit is placed inside a magnetic field, the magnetic flux lines exert a force on the semiconductor plate causing electrons and positive poles to deflect to either side of the plate. The movement of the charge carriers is because of the magnetic force that they experience. So, if we place a voltage meter between the two sides of the plate, we will get some voltage depending on the magnetic field strength and its direction [26].

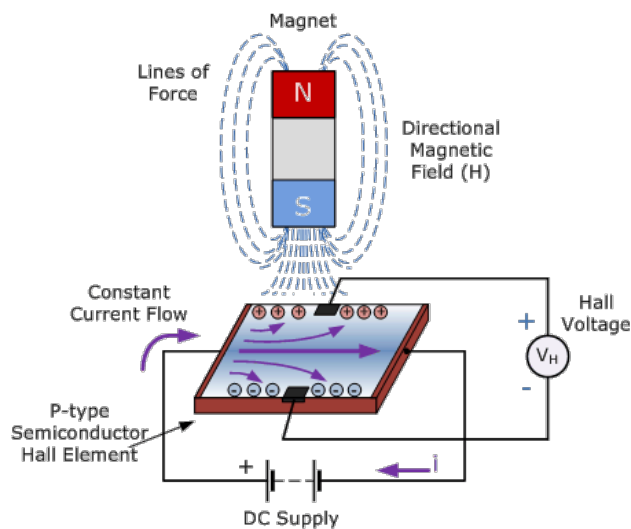


Figure 31 Hall effect based magnetometer [27].

3.3 Orientation

In order to calculate the orientation of the sensor we need to discuss some terms that are used generally. First of all, orientation is the heading of the sensor, we need to know at any time how many degrees in each axis our sensor has tilted. In the 3.3.1 we introduce the rotation matrices and then we will present two options on how to calculate orientation. We will also see the reasons that lead us to choose one of them.

3.3.1 Rotation matrices

Let's consider a 3×3 rotation matrix that is a special orthogonal group we can present it as follows

$$R = [\hat{x} \hat{y} \hat{z}] \in SO(3)$$

Each column of the vector is a 3D unit vector meaning

- $\hat{x}, \hat{y}, \hat{z} \in \mathbb{R}^3$
- $\|\hat{x}\| = \|\hat{y}\| = \|\hat{z}\| = 1$

All special orthogonal group has the following properties $RR^T = R^T R = I$, $\|R\| = 1$ and $\det(R) = 1$ where I is the identity matrix meaning its diagonal has ones and the rest of the matrix has zeros. The term special orthogonal group define that only matrices with $\det(R) = 1$ are treated as rotations. Now let's see an example, consider that we have two frames a and b and a vector x expressed at b frame can be rotated at a frame as mentioned below

$$x^a = R_b^a x^b \quad \text{where } R_b^a \text{ denotes that we are at frame } b \text{ and we want to rotate at frame } a$$

oppositely we have,

$$x^b = (R_b^a)^T x^a = R_a^b x^a$$

With the rotation matrix we can represent a unique description of orientation.

3.3.2 Euler angles

Euler angles are a way to represent an 3D orientation of an object using a combination of three rotations about different axes. Let's use a (z, y, x) coordinate system that first rotates at angle ψ around z -axis (yaw rotation), afterwards at angle θ around y -axis (pitch rotation) and finally at an angle ϕ around x -axis (roll rotation). We want to rotate our object from the 'inertial frame', that as mentioned on 3.2.1 it's a frame that is earth-fixed and does not rotate

with the rest of the universe, to the body frame that its axes are aligned with the sensor. We will use another two coordinate frames v_1 and v_2 in order to help us reach to the body frame.

3.3.2.1 Yaw rotation

The figure 32 shows the object at ‘inertial frame’ that is rotated at an angle ψ and attain v_1 frame. This rotation can be written as follows

$$R_I^{v_1}(\psi) = \begin{pmatrix} \cos(\psi) & \sin(\psi) & 0 \\ -\sin(\psi) & \cos(\psi) & 0 \\ 0 & 0 & 1 \end{pmatrix}$$



Figure 32 Yaw rotation

3.3.2.2 Pitch rotation

Now we will rotate from v_1 frame to v_2 frame at an angle θ around y -axis as shown in the figure 33. The rotation can be written as follows

$$R_{v_1}^{v_2}(\theta) = \begin{pmatrix} \cos(\theta) & 0 & -\sin(\theta) \\ 0 & 1 & 0 \\ \sin(\theta) & 0 & \cos(\theta) \end{pmatrix}$$

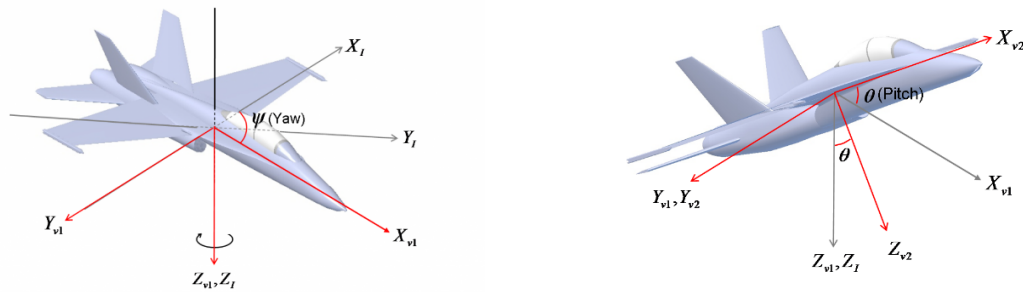


Figure 33 Pitch rotation

The rotation for moving from inertial frame to v2 frame is the multiplication of yaw matrix by pitch matrix $R_I^{v2}(\psi, \theta) = R_I^{v1}(\psi) R_{v1}^{v2}(\theta)$

3.3.2.3 Roll rotation

Lastly, we rotate from v2 frame to the desired body frame by an angle φ around x-axis as shown in figure 34. The rotation matrix from v2 frame to body frame is given by

$$R_{v2}^b(\varphi) = \begin{pmatrix} 1 & 0 & 0 \\ 0 & \cos(\varphi) & \sin(\varphi) \\ 0 & -\sin(\varphi) & \cos(\varphi) \end{pmatrix}$$



Figure 34 Roll rotation

So, the orientation from inertial frame to body frame is given by

$$R_I^b(\psi, \theta, \varphi) = R_I^{v1}(\psi) R_{v1}^{v2}(\theta) R_{v2}^b(\varphi)$$

After we multiply the matrices the complete rotation can be written as

$$R_I^b(\psi, \theta, \varphi) = \begin{pmatrix} \cos(\theta) \cos(\psi) & \cos(\theta) \sin(\psi) & -\sin(\theta) \\ \sin(\varphi) \sin(\theta) \cos(\psi) - \cos(\varphi) \sin(\psi) & \sin(\varphi) \sin(\theta) \sin(\psi) + \cos(\varphi) \cos(\psi) & \sin(\varphi) \cos(\theta) \\ \cos(\varphi) \sin(\theta) \cos(\psi) + \sin(\varphi) \sin(\psi) & \cos(\varphi) \sin(\theta) \sin(\psi) - \sin(\varphi) \cos(\psi) & \cos(\varphi) \cos(\theta) \end{pmatrix}$$

So, Euler angles are extremely helpful because we obtain three angles that represent our orientation by yaw, pitch and roll, but they suffer from gimbal lock. Gimbal lock occurs when the pitch angle is 90 degrees or -90 degrees, then yaw and roll are exactly the same thing causing the sensor to move in exactly the same fashion. Therefore, Euler angles are preferred to use when the application does not require the object to tilt at 90 degrees on y-axis. This is a fundamental problem of Euler Angles and it can only be solved by switching to a different representation method. The other method that will be presented is called quaternions and although the output is valid when Euler angles are not, they are more complex and harder to understand [28].

3.3.3 Unit Quaternions

Quaternions were first introduced by Hamilton, more details about quaternions at [29]. Unit quaternions are quaternions that are used to provide a different measurement technique on orientation, they are a four-element vector that can be used to define any rotation in a 3D coordinate system but they are more complicated and harder to understand.

Let's consider the following frames as were presented in 3.3.2, we want to rotate from the 'inertial frame' to the 'body frame', q_i^b is a unit quaternion that encodes that rotation and it can be written as follows

$$q_i^b = (a \ b \ c \ d)^T, \quad q_i^b \in \mathbb{R}^4, \quad \|q_i^b\| = 1 \quad \text{and} \quad a^2 + b^2 + c^2 + d^2 = 1$$

where T is the transpose vector, the b , c and d elements are called the vector part of the quaternion and can be translated as a vector on which rotation should be performed. The a element is the scalar part and it indicates the amount of rotation that should be performed on the vector part. So, if we want to rotate at an angle θ and the vector $(x \ y \ z)^T$ is a vector that represents the axis of rotation then the elements a , b , c , d can be calculated as follows

$$\begin{pmatrix} a \\ b \\ c \\ d \end{pmatrix} = \begin{pmatrix} \cos\left(\frac{\theta}{2}\right) \\ x\sin\left(\frac{\theta}{2}\right) \\ y\sin\left(\frac{\theta}{2}\right) \\ z\sin\left(\frac{\theta}{2}\right) \end{pmatrix} \quad (1)$$

The quaternion q_i^b can be used to rotate a random 3 element vector from the inertial frame to body frame using the following equation using the upcoming operation

$$v_b = q_i^b \begin{pmatrix} 0 \\ v_i \end{pmatrix} (q_i^b)^{-1}$$

A vector can be rotated by treating it like a quaternion with zero real part and multiplying it by the quaternion and its inverse, that is the reason when we want to rotate at angle θ we use the half the angle at (1). The inverse of a quaternion is equal to its conjugate, which mean that all the vector elements are negated. The rotation also uses multiplication of quaternions, therefore let's define two quaternions with the form

$q_1 = (a_1 \ b_1 \ c_1 \ d_1)^T$ and $q_2 = (a_2 \ b_2 \ c_2 \ d_2)^T$. The product q_1q_2 is given by

$$q_1q_2 = \begin{pmatrix} a_1a_2 - b_1b_2 - c_1c_2 - d_1d_2 \\ a_1b_2 + b_1a_2 + c_1d_2 - d_1c_2 \\ a_1c_2 - b_1d_2 + c_1a_2 + d_1b_2 \\ a_1d_2 + b_1c_2 - c_1b_2 + d_1a_2 \end{pmatrix}$$

In order to rotate a vector, multiplication of two quaternions is required. A different method is to build a 3 by 3 rotation matrix to perform the rotation in a single matrix multiply operation. The rotation from the inertial frame to body frame using the quaternion elements is defined as

$$R_i^b(q_i^b) = \begin{pmatrix} 1 - 2(c^2 + d^2) & 2(bc - ad) & 2(ac + bd) \\ 2(bc + ad) & 1 - 2(b^2 + d^2) & 2(cd - ab) \\ 2(bd - ac) & 2(ab + cd) & 1 - 2(b^2 + c^2) \end{pmatrix}$$

Therefore, now the rotation from inertial frame to body frame can be performed using the matrix multiplication

$$v_b = R_i^b(q_i^b)v_i$$

[30]

Quaternions can also be used to calculate ψ , θ , φ angles from 3.2.2. but unfortunately, it does not negate the gimbal lock problem. The converse from quaternions to Euler angles is given by

$$\begin{pmatrix} \varphi \\ \theta \\ \psi \end{pmatrix} = \begin{pmatrix} \arctan \frac{2(ab + cd)}{1 - 2(b^2 + c^2)} \\ \arcsin 2(ac - db) \\ \arctan \frac{2(ad + bc)}{1 - 2(c^2 + d^2)} \end{pmatrix}$$

[31]

Unit quaternions are very critical because they are used in this thesis in order to calculate the orientation through an algorithm that is called AHRS more details in [32], [33]. They do not suffer from gimbal lock and can represent any rotation, but they are more complicated and the mathematics are harder than Euler angles. Rotation matrices will be constructed after the use of AHRS algorithm for that reason understanding background theory and some mathematic terms is essential as we proceed to the code that was used.

3.4 Position

The calculation of position as discussed at 3.1 can be plain simple because from uncomplicated mathematics and physics we know that in order to get velocity we integrate acceleration and to get position the integration of velocity is required [34]. Let's consider our sensor acceleration can be described with a function that is time related $a(t)$. Since the time derivative of the velocity function is acceleration,

$$\frac{d}{dt}v(t) = a(t)$$

We can take the indefinite integral of both sides leading to,

$$\int \frac{d}{dt}v(t)dt = \int a(t)dt + C_1$$

where C_1 is a constant of integration. Since

$$\int \frac{d}{dt}v(t)dt = v(t)$$

the velocity is given by

$$v(t) = \int a(t)dt + C_1.$$

Same way, the time derivative of the position function is the velocity function,

$$\frac{d}{dt}x(t) = v(t).$$

So, we can find that,

$$x(t) = \int v(t)dt + C_2.$$

We notice that in fact the accelerometer does not measure linear acceleration. It picks up forces applied on the proof mass and measure the displacement of the mass to calculate

acceleration. The force of gravity is always picked up by the accelerometer and is taken as acceleration. An accurate attitude of the sensor has to be estimated in order to subtract the gravity factor on all three axes so as to obtain an estimate of linear acceleration. Otherwise small errors in the measurement of acceleration are integrated into progressively larger errors in velocity, which are compounded into still greater errors in position. Since the new position is calculated from the previous calculated position and the measured acceleration and angular velocity, these errors accumulate roughly proportionally to the time since the initial position was input [35]. This is known as the notorious integration drift problem of inertial navigation system, which we try to reduce by using some filters. Calculation of position was the toughest part because the data from the accelerometer have some noise and the integration of that can cause a linear error in velocity and quadratic error in position.

3.5 Hardware Implementation

In this paragraph the hardware implementation will be presented. We did not want to complicate our setup so an Arduino Uno was used and our IMU sensor was placed on the board. The communication between the sensor and the Arduino was the I2C protocol. Apart from the simplicity of the circuit the cost was the primal concern, the mpu9250 by Sparkfun costs only 14.95 \$ [36] and the Arduino Uno was low cost as well approximately 10 \$.

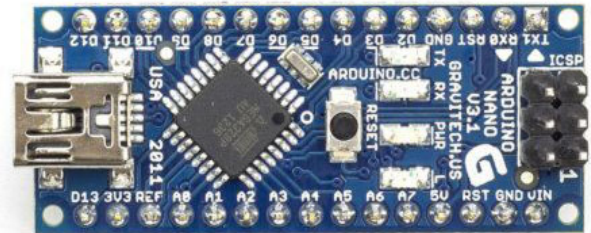
3.5.1 Arduino

Arduino Uno was first used as a processing unit and even though it has smaller I/O capabilities than other Arduino's it was powerful enough to process our data. It contains an ATmega328p microcontroller, it has 14 digital input/output pins (of which 6 can be used as PWM outputs), 6 analog inputs, a 16 MHz quartz crystal, a USB connection, a power jack, an ICSP header and a reset button. In order to reduce size an Arduino Nano was used, that has also an ATmega328p (Figure 35 b). As a power supply we did not use a common battery but a USB connected to the computer. Not only the ease of programming on the Arduino platform but

also the fact that there is a helpful forum that helps with some questions makes the Arduino a suitable processing unit. We can see the board in figure 35 (a).



(a)



(b)

Figure 35 (a) Arduino Uno board (b) Arduino Nano board

3.5.2 MPU9250

The sensor we used was the MPU9250 by Sparkfun. It contains a 3-axis accelerometer with programmable sensitivity $\pm 2g$, 4, 8 or 16g gives you the freedom of deciding according to the project what sensitivity you want. Lower the sensitivity the more accuracy so the sensitivity was set at $\pm 2g$. It also contains a 3-axis gyroscope with programmable sensitivity ± 250 , 500, 1000, or 2000 degrees per second or (dps). Gyroscope sensitivity was set at ± 250 degrees per second. Both gyroscope and accelerometer can reach a sample rate at 1kHz and they both contains capacitors inside. It also contains a 3-axis magnetometer the AK8963 that works under the Hall effect and it can reach up to 8 Hz repetition rate, more details about the mpu9250 can be found at [37]. The mpu9250 has many features and it can communicate to a system processor using SPI or a I2C serial communication. For the communication we used

the I2C protocol. It also has eleven pins of which we used four of them. The pins we used was the SCL, SDA, VDD, GND, we can see the sensor at Figure 36.



Figure 36 (a) Top view of sensor (b) Bottom view of sensor [38]

3.5.3 I2C protocol

As mentioned before for our serial communication we used the I2C protocol. I2C Protocol is a way of serial communication between different devices to exchange their data with each other. It is a half-duplex bi-directional two-wire bus system for transmitting and receiving data between masters (M) and slaves (S). These two wires are Serial clock line or SCL and Serial data line or SDA. Masters and Slaves play important role in I2C communication. Master is the one which initiates a communication, generates a clock and terminates the communication and Slave is the one which is handled by master and acts according to the master command. It can also be possible that multiple masters can communicate with multiple slaves [39]. In figure 37 we can see an example of a I2C protocol where a single master communicates with multiple slaves.

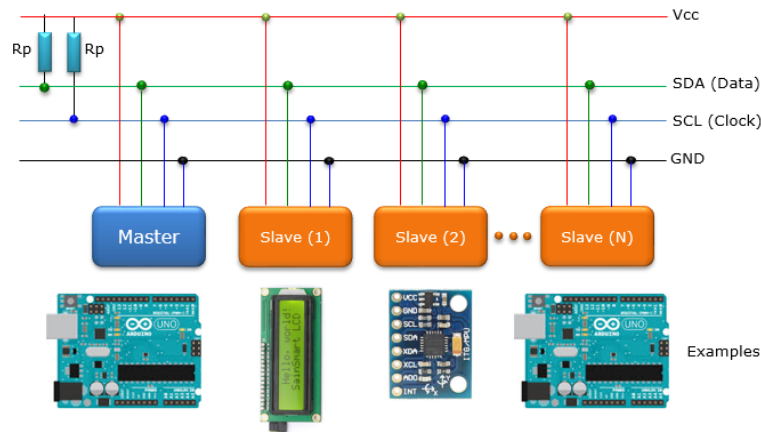


Figure 37 An example of connection between multiple devices with I2C protocol [40]

3.5.4 Our circuit

The circuit that we build is shown at figure 39. First, we connected the pin VDD pin of MPU9250 at the 5 volts of the Arduino and the GND pin of the sensor at the GND of Arduino. Then we connected the SCL and SDA of the sensor with the SCL and SDA of Arduino accordingly. To connect pins between Arduino and the sensor we used four male to male cables. For the supply of Arduino, we decided not use batteries but a USB directly connected to a laptop. Arduino board was selected because for our experiment it is good enough to process our data and because Sparkfun provides plenty of help and friendly environment between customer and provider. The simplicity of the sensor makes it very easy for users to connect it on Arduino and start developing code according to their project.

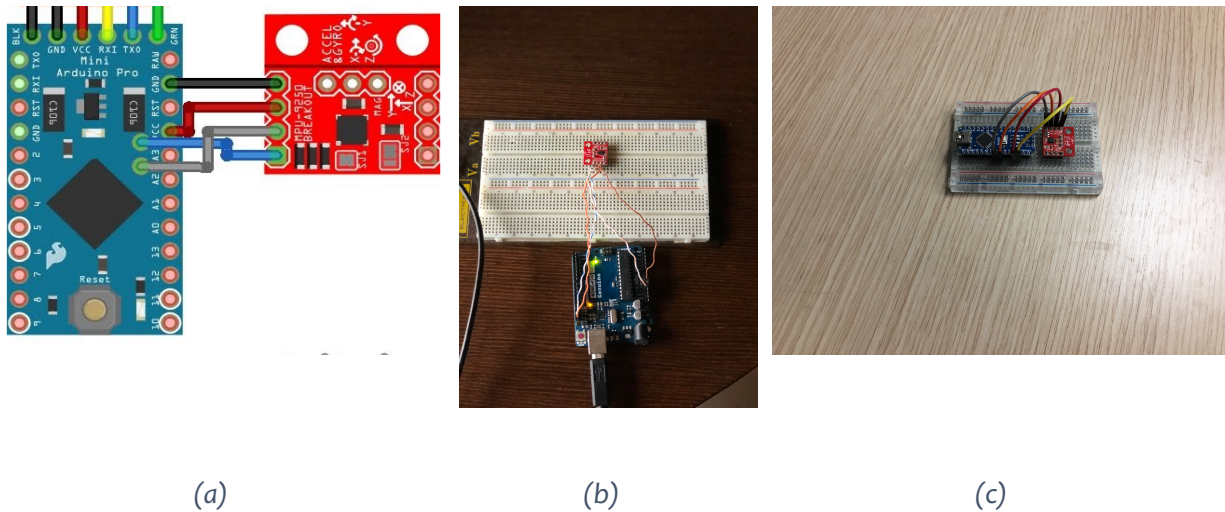


Figure 38 Hookup between MPU9250 and Arduino [38] (a) zoomed in circuit (b) zoomed out circuit (c) circuit with Arduino Nano

3.5.5 Unused hardware

As was mentioned on 3.2.2 MPU9250 contains a 3-axis magnetometer. Usually the use of magnetometer is to find the heading of sensor or the yaw angle, it is often called absolute orientation and it is with respect to magnetic north making our sensor work like a real compass. The magnetometer was not used at this project that's why we will not see the values on the code that was developed.

3.6 Software Implementation

The software will be organized as follows, first we will show the general idea of how we get position through accelerometer and gyroscope data, then we will present more details on how we achieved each step of the general idea. As we see in figure 39, we first implement gyroscope and accelerometer data into an AHRS algorithm we will see more details about this algorithm when we will present step by step the code that we developed.

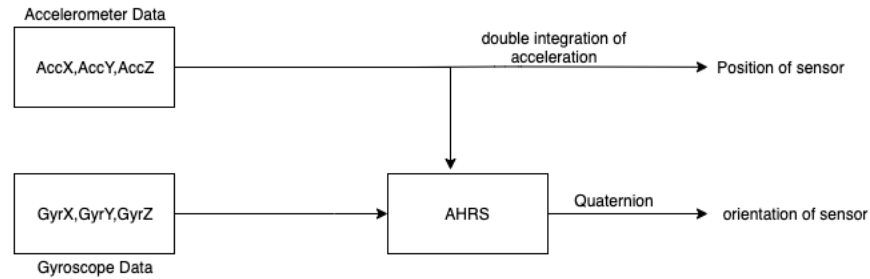


Figure 39 General diagram of position and orientation estimation

3.6.1 AHRS

Mems IMUs are vulnerable to many kinds of noises and errors. Accelerometers are sensitive to attitude changing, impact forces and vibrations while gyroscopes are sensitive to temperature change and slow changing bias. To sum up accelerometers have poor dynamic features and gyroscopes have poor static features which means that we trust the accelerometer for the long term or for low frequencies and we trust gyroscope for the short-term changes or high frequencies. Therefore, we use the AHRS algorithm to fuse the data from different sensors in order to gain the advantages of each of them, so we get a better prediction of the actual status of the sensor. There are two main categories of AHRS, the one is based on Kalman filter and the other is based on complementary filter. The algorithm we chose was developed by Mahony and it is called Explicit Complementary Filter more details at [41], [42]. In figure 40 we can see the block diagram of the filter or AHRS.

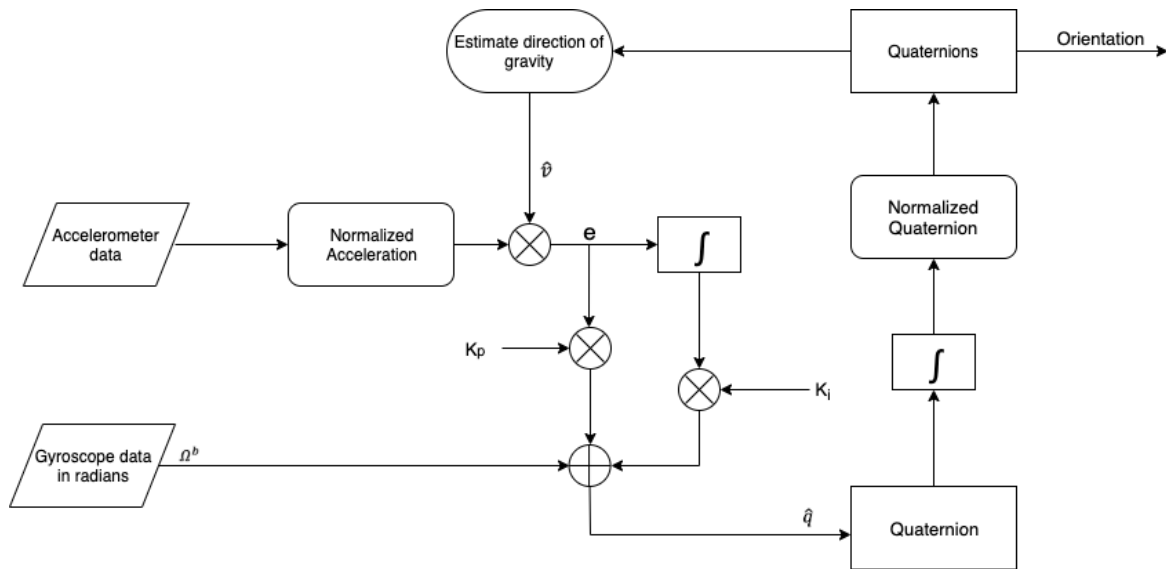


Figure 40 Block diagram of AHRS

The algorithm can be summarized in the following steps:

1. At the beginning of the algorithm we initialize the quaternion with a value $[1, 0, 0, 0]$, that value can be translated as a unit quaternion and we have zero rotation. Also K_i , K_p and sampling frequency are defined.
2. Data input: a set of acceleration and gyroscope data in radians is fed in and acceleration data are normalized
3. Estimated gravity direction: estimate of gravity direction using the current quaternion q is calculated using the following formula [43],

$$\hat{v} = \begin{bmatrix} 2(q_1q_3 + q_0q_2) \\ 2(q_2q_3 + q_0q_1) \\ q_0^2 - q_1^2 - q_2^2 + q_3^2 \end{bmatrix}$$

4. Error calculation: The error can be calculated by taking the cross product of estimated gravity and true gravity. The true gravity is given by the normalized accelerometer, so the error between estimated direction of gravity from gyroscope and from accelerometer is given by,

$$e = acc_{norm} \times \hat{v}$$

5. Data fusion: error is calculated to reduce bias in gyroscope data in the next loop. Error is applied as a feedback term with two adjustable coefficients: the proportional gain K_p and the integral gain K_i , which forms a PI controller,

$$\bar{\Omega}^b = \Omega^b + K_p e + K_i \int e dt$$

6. Compute rate of change of quaternion: according to differentiation formula of quaternion, we get,

$$\hat{q}' = \frac{1}{2} \hat{q} \otimes p(\bar{\Omega}^b)$$

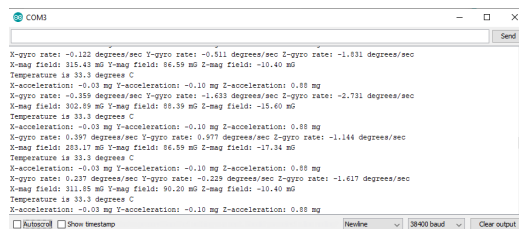
Where $p(\bar{\Omega}^b) = (0, \bar{\Omega}^b)$ because we need same length of matrices in order to get the product and \hat{q} is the quaternion of last iteration.

7. Estimate orientation: now that the differentiation of the quaternion in last iteration is calculated, simply integrate it and yield estimated quaternion, namely orientation. Then the quaternion of this iteration is normalized.

Repeat from **step 2** in order to keep tracking of orientation.

3.6.2 Algorithm we used

Before we start getting into details about the algorithm, we first need to state that the sensor data was sent from Arduino and processed in MATLAB. In figure 41 we can see the raw data from the sensor displayed on the Arduino serial monitor. The raw data was logged into a csv file and then processed in MATLAB, this was done with help of a program called tera term. TeraTerm is an open source, free, software implemented, terminal emulator program [44]. It has the option on showing the data in a terminal window as shown in figure 42 coming from the selected port, but the main reason that it was used was because it can log the data into a .csv file. In the figure 43 we can see the data flow.

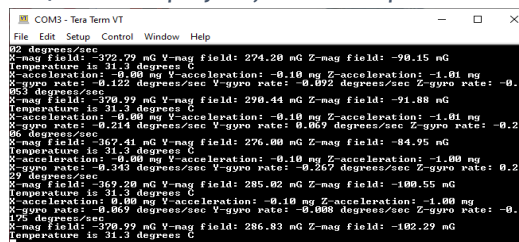


```

COM3
X-gyro rate: 0.122 degrees/sec Y-gyro rate: -0.511 degrees/sec Z-gyro rate: -1.831 degrees/sec
X-mag field: 315.43 mG Y-mag field: 86.59 mG Z-mag field: -10.40 mG
Temperature is 33.3 degrees C
X-acceleration: -0.03 mg Y-acceleration: -0.10 mg Z-acceleration: 0.88 mg
X-gyro rate: -0.355 degrees/sec Y-gyro rate: -1.433 degrees/sec Z-gyro rate: -2.731 degrees/sec
X-mag field: 302.89 mG Y-mag field: 85.39 mG Z-mag field: -15.60 mG
Temperature is 33.3 degrees C
X-acceleration: -0.03 mg Y-acceleration: -0.10 mg Z-acceleration: 0.88 mg
X-gyro rate: 0.397 degrees/sec Y-gyro rate: 0.977 degrees/sec Z-gyro rate: -1.144 degrees/sec
X-mag field: 283.17 mG Y-mag field: 86.59 mG Z-mag field: -17.34 mG
Temperature is 33.3 degrees C
X-acceleration: -0.03 mg Y-acceleration: -0.10 mg Z-acceleration: 0.88 mg
X-gyro rate: 0.237 degrees/sec Y-gyro rate: -0.223 degrees/sec Z-gyro rate: -1.617 degrees/sec
X-mag field: 311.85 mG Y-mag field: 90.20 mG Z-mag field: -10.40 mG
Temperature is 33.3 degrees C
X-acceleration: -0.03 mg Y-acceleration: -0.10 mg Z-acceleration: 0.88 mg
 Autoclear  Show timestamp   

```

Figure 41 Data displayed from serial port in Arduino.



```

COM3 - Tera Term VT
File Edit Setup Control Window Help
92 degrees/sec
X-mag field: 322.29 mG Y-mag field: 274.20 mG Z-mag field: -90.15 mG
Temperature is 31.3 degrees C
X-acceleration: -0.08 mg Y-acceleration: -0.10 mg Z-acceleration: -1.01 mg
X-gyro rate: -0.122 degrees/sec Y-gyro rate: 0.092 degrees/sec Z-gyro rate: -0.
054 degrees/sec
X-mag field: 370.99 mG Y-mag field: 290.44 mG Z-mag field: -91.88 mG
Temperature is 31.3 degrees C
X-acceleration: -0.08 mg Y-acceleration: -0.10 mg Z-acceleration: -1.01 mg
X-gyro rate: -0.214 degrees/sec Y-gyro rate: 0.069 degrees/sec Z-gyro rate: -0.2
96 degrees/sec
X-mag field: 367.41 mG Y-mag field: 276.00 mG Z-mag field: -84.95 mG
Temperature is 31.3 degrees C
X-acceleration: -0.08 mg Y-acceleration: -0.10 mg Z-acceleration: -1.00 mg
X-gyro rate: -0.343 degrees/sec Y-gyro rate: -0.267 degrees/sec Z-gyro rate: 0.2
29 degrees/sec
X-mag field: 369.20 mG Y-mag field: 285.02 mG Z-mag field: -100.55 mG
Temperature is 31.3 degrees C
X-acceleration: 0.00 mg Y-acceleration: -0.10 mg Z-acceleration: -1.00 mg
X-gyro rate: -0.069 degrees/sec Y-gyro rate: -0.008 degrees/sec Z-gyro rate: -0.
174 degrees/sec
X-mag field: 370.99 mG Y-mag field: 286.83 mG Z-mag field: -102.29 mG
Temperature is 31.3 degrees C

```

Figure 42 Data displayed from serial port in TeraTerm.



Figure 43 Data flow

In the figure 44 we can see the UML diagram that was used for assigning the data from .csv file into variables. A UML diagram is used to comprehend the inheritance between the classes that were developed.

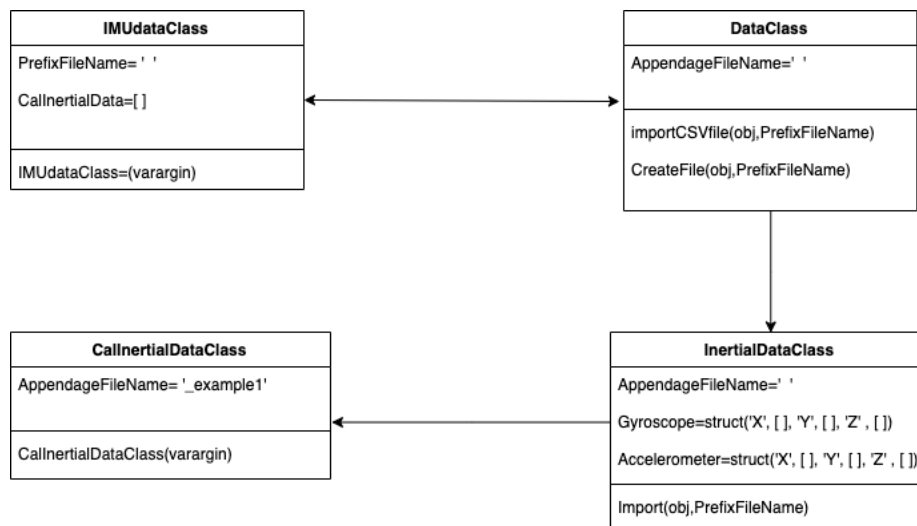


Figure 44 UML diagram for assigning the data from .csv into variables.

All the classes inherit from handle class, which is the class that any class needs to inherit from. It is similar to abstract class in java.

DataClass checks if the file exists or not. If the file does not exist it outputs an error message otherwise it stores all the data in a variable.

InertialDataClass inherits from DataClass and uses the data coming from the class in order to store them into six variables: AccelerometerX, AccelerometerY, AccelerometerZ, GyroscopeX, GyroscopeY and GyroscopeZ.

CallInertialDataClass inherits from InertialDataClass. It adds the property “sample rate” to data object. On the other side, IMUdataClass takes in a file and set up a data object with complete properties like sample rate.

Now that we have explained how we store the data coming from the .csv file are stored into variables and how AHRS works we can present the algorithm that was developed. In figure 45 we can see the block diagram of the algorithm.

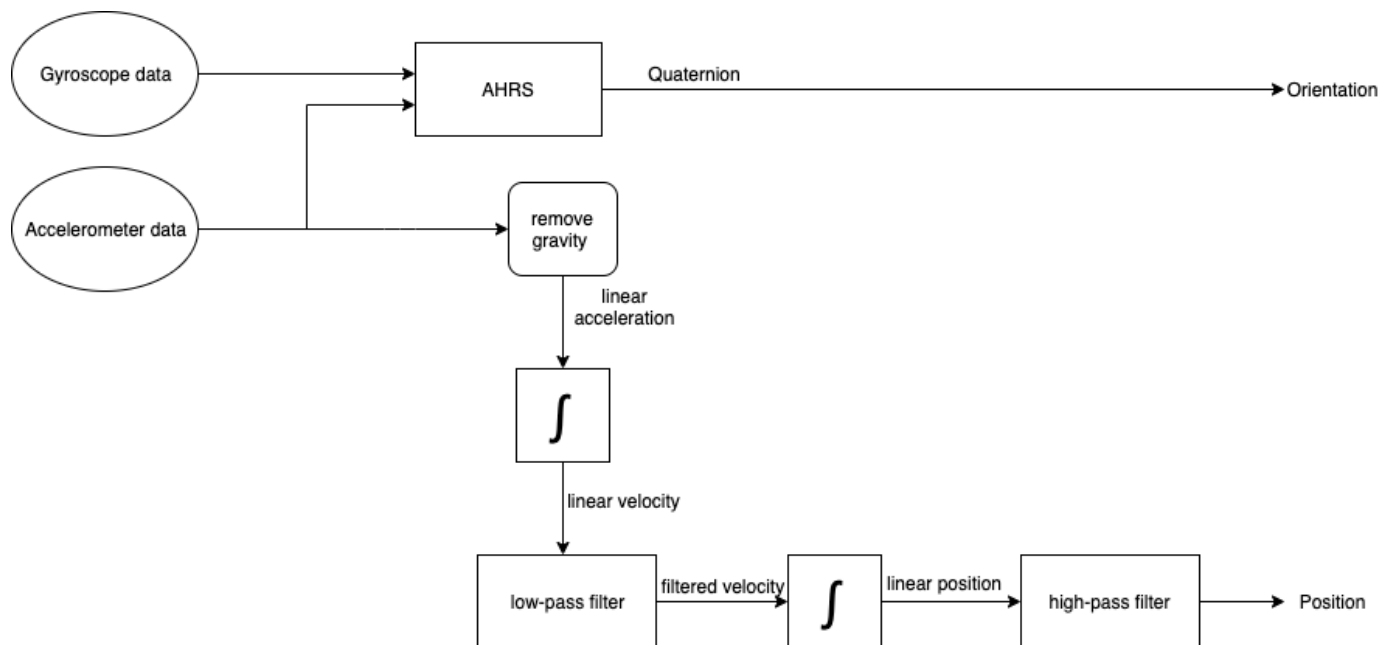


Figure 45 Block diagram of algorithm

The algorithm contains the following steps:

Step 1: The accelerometer and gyroscope data are inserted in AHRS that contains the explicit complementary filter as was presented at 3.4.1. The output is a quaternion that represents the orientation.

Step 2: The gravity from acceleration is removed so we get linear acceleration so we can integrate.

Step 3: Integrate linear acceleration to get linear velocity.

Step 4: Use a first order Butterworth low-pass filter to remove noise from velocity.

Step 5: Integrate linear velocity to get linear position

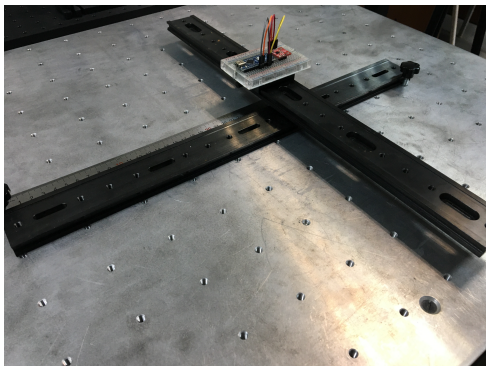
Step 6: Use a first order Butterworth high-pass filter to remove drift from position

So, from **Step 6** we obtain the displacement on all three axes and from **Step 1** we obtain the orientation estimation. Notice that each time we use integration a drift reduction method is used. In AHRS we use a PI controller that reduce the gyroscope drift. In velocity level we used a low-pass filter to reduce noise of acceleration and in position level we used a high-pass filter to erase drift caused by tiny errors from the two lower levels. The filters as we see are essential if they were not used it would cause errors on our results.

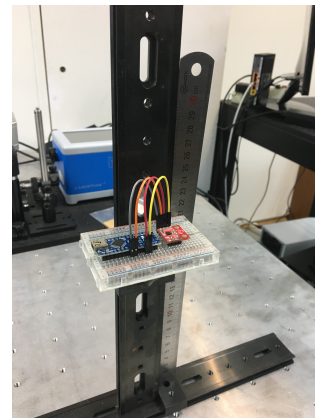
CHAPTER 4

4.1 Experimental results

In this chapter we are going to see some experimental results that were taken in translational XYZ rail stage as shown in figure 46. At first, we are going to start with some raw data coming from accelerometer and gyroscope. In figure 47 we can see the data coming from accelerometer and gyroscope as the sensor remains stationary. The frequency was set at 16 Hz. At the accelerometer figure the Z axis shown as blue is at 1g even though the sensor remains stationary, the reason is that as was mentioned accelerometers measure not only external applied forces but also gravitational acceleration. At the gyroscope figure all the values remain at zero.



(a)



(b)

Figure 46 (a) XY rail translator (b) Z rail

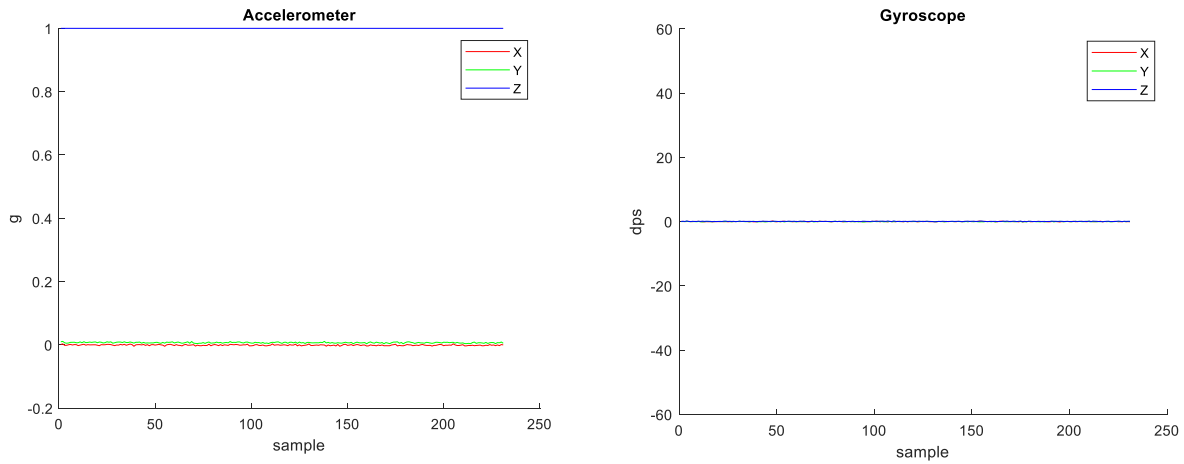


Figure 47 Plots of accelerometer and gyroscope when sensor is stationary

At next, we will present the figures when we move the sensor at 60cm to X axis. At figure 48 upper left the accelerometer data are displayed at upper middle the gyroscope data. At upper right we can see the figure that we remove gravity accelerometer data and convert them in meters per second squared. At lower left we can see the velocity after acceleration integration. Lower middle a low pass filter is applied and we can see that the noise has been removed effectively. Lower right the position of the sensor is shown after we integrate velocity and filter position in order to remove drift. The position that sensor displays after our algorithm is **0.5886m**. We can observe that the position tends to return at zero, this is happening because acceleration is returning to its initial values when no force is applied to the sensor. So, position will always return to zero when we are not moving the sensor.

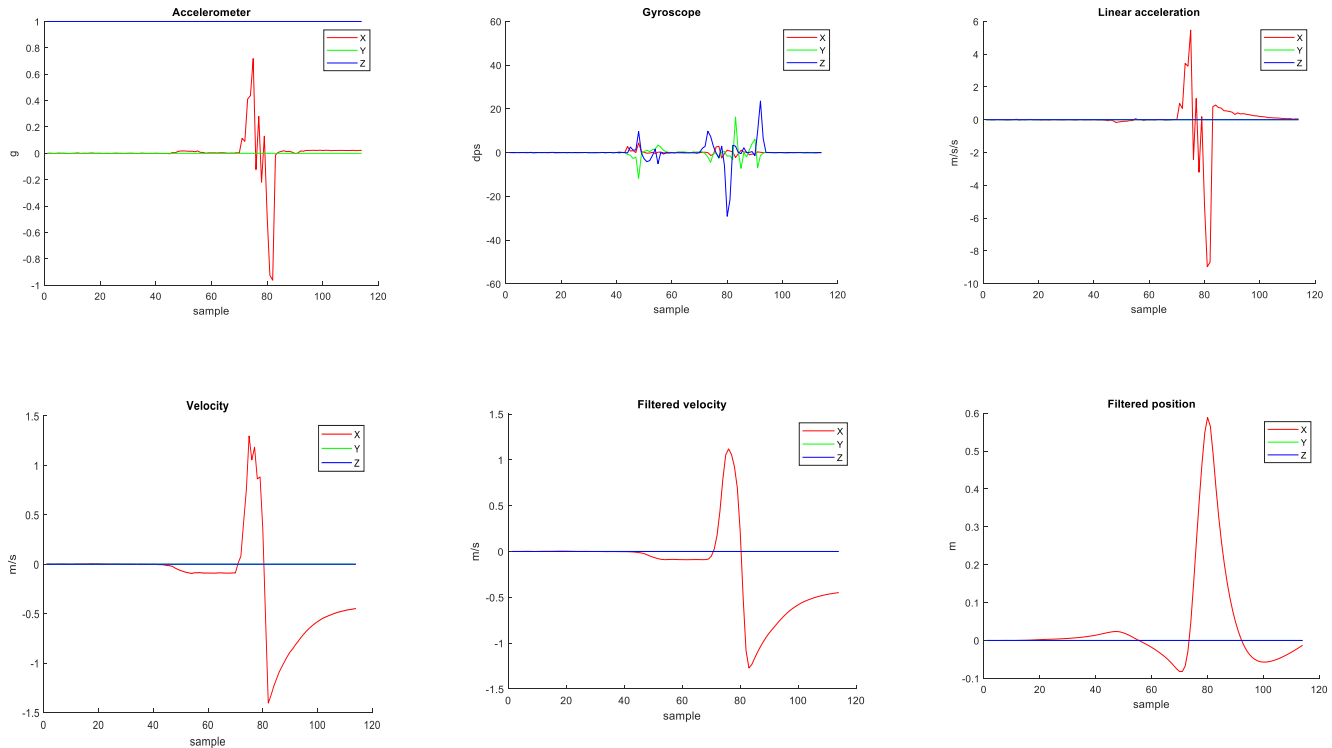


Figure 48 Plots when moving sensor 60cm at the X axis. Low right the position is displayed.

With the same principle as before we will present the figures when we move the sensor at Y axis for 40cm. As shown in figure 49 lower right the position we obtain is **0.4091m**. If we compare the velocity plot with the filtered velocity, we can realize that firstly we remove any noise but secondly the velocity starts to drift (Fig. 49 lower left) because as we mentioned before there is an error caused by integrating. In the current experiment there were not enough samples but as the time was passing by velocity would not return to zero but it would keep having the 0.2 value (Fig 49 lower left and middle). To overcome this problem, we high pass filter the position.

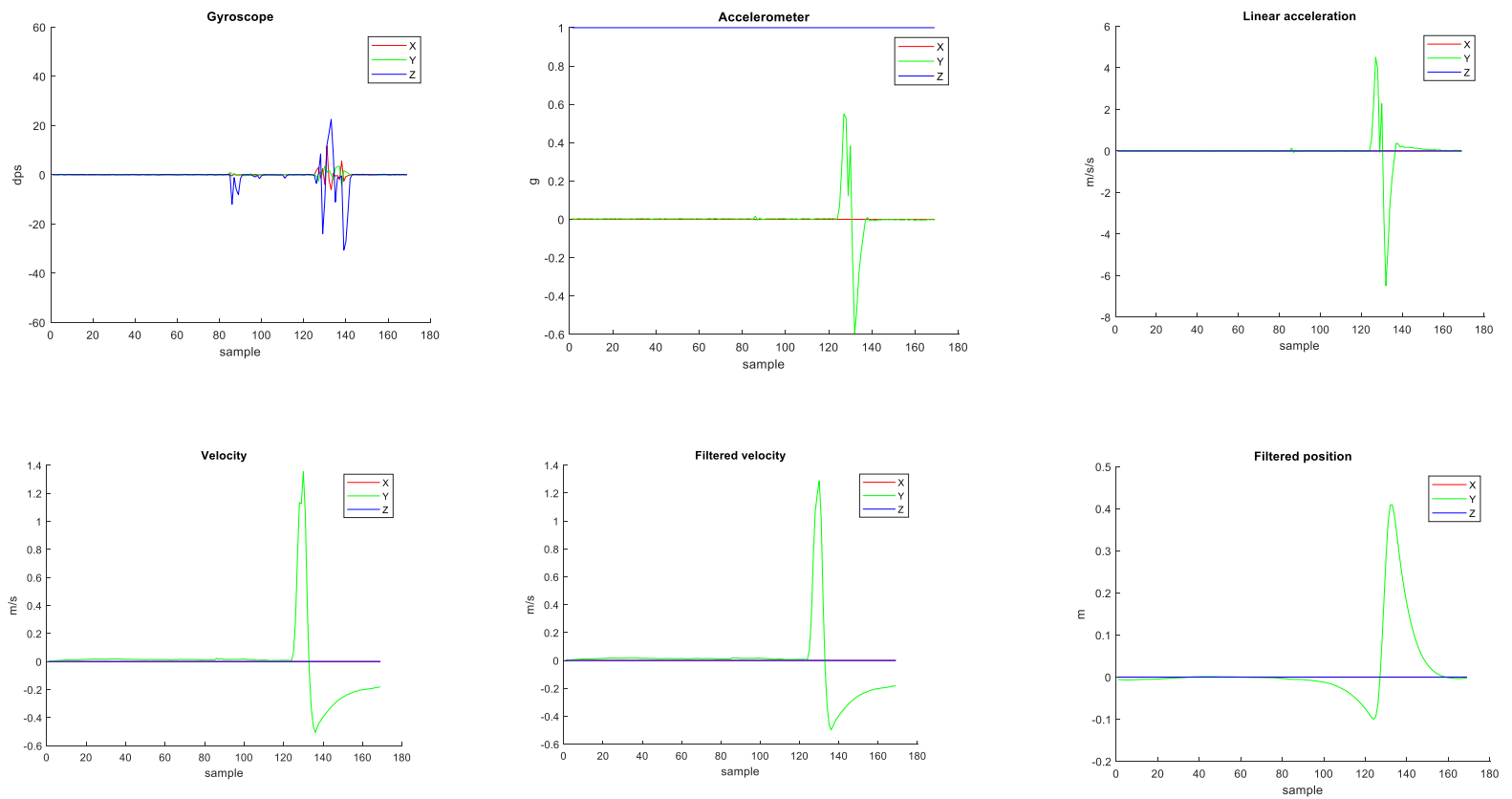


Figure 49 Plots when moving the sensor 40cm to Y axis. Lower right the position is displayed

Now figures will be displayed when we move the sensor at X, Y axis at a distance of 30cm together. At figure 50 lower right we can see the position that specifically is $X=0.3075m$ and $Y=0.2922m$.

Next, we move the sensor at 30cm up (along the Z axis). The results are shown in figure 51 where we can see the position diagram at lower right. Exactly the position is **0.3056m**, at accelerometer data that Z axis (blue line) senses some movement that is around 1g, then at

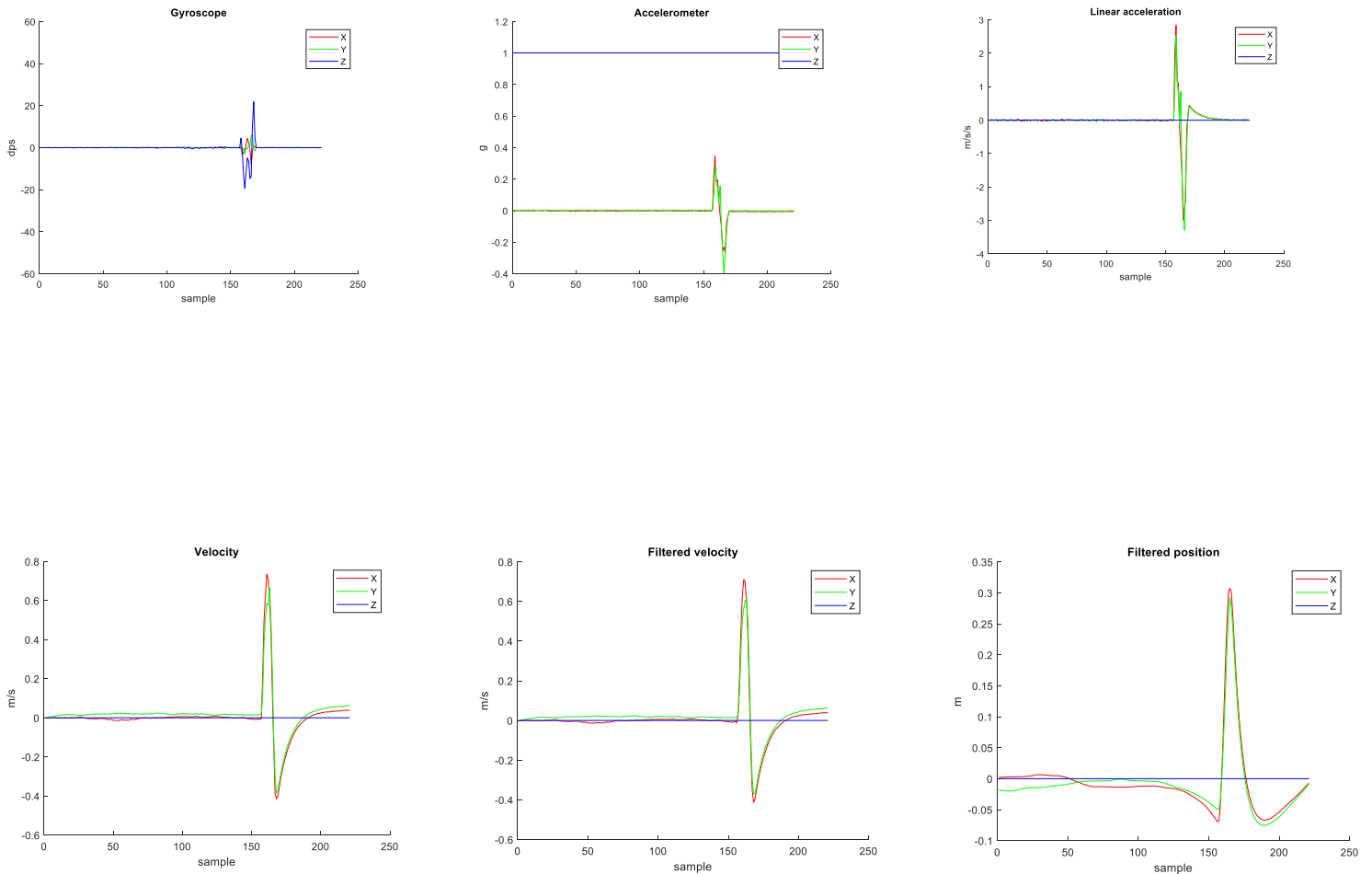


Figure 50 Plots when moving the sensor at 30cm at XY axis. Lower right the position is displayed.

linear acceleration we can realize that the graph is displaced at zero. The reason is when we move the sensor at Z axis, as we mentioned before Z axis senses gravity, we want to remove the gravity in order to be able to integrate acceleration. If gravity was not removed that would cause huge error.

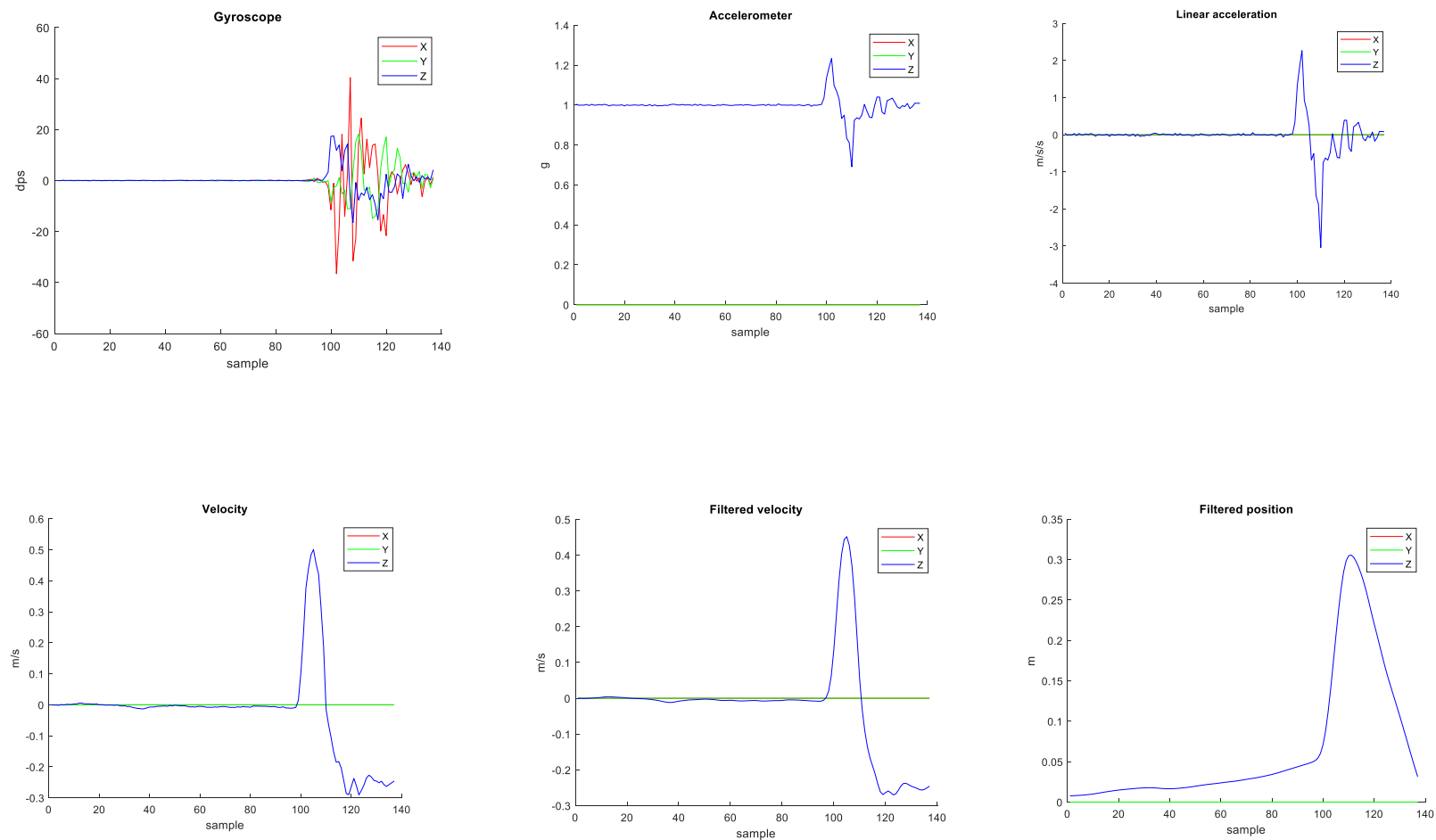


Figure 51 Plots when moving the sensor 30cm at Z axis. Lower right the position is displayed.

Lastly, we moved the sensor at all axis at the same time at 30cm on each axis. The final results are shown in figure 52, where at bottom right we can see the position of X, Y and Z. The exact value at X is **0.3088m**, at Y is **0.2967m** and at Z is **0.3046m**.

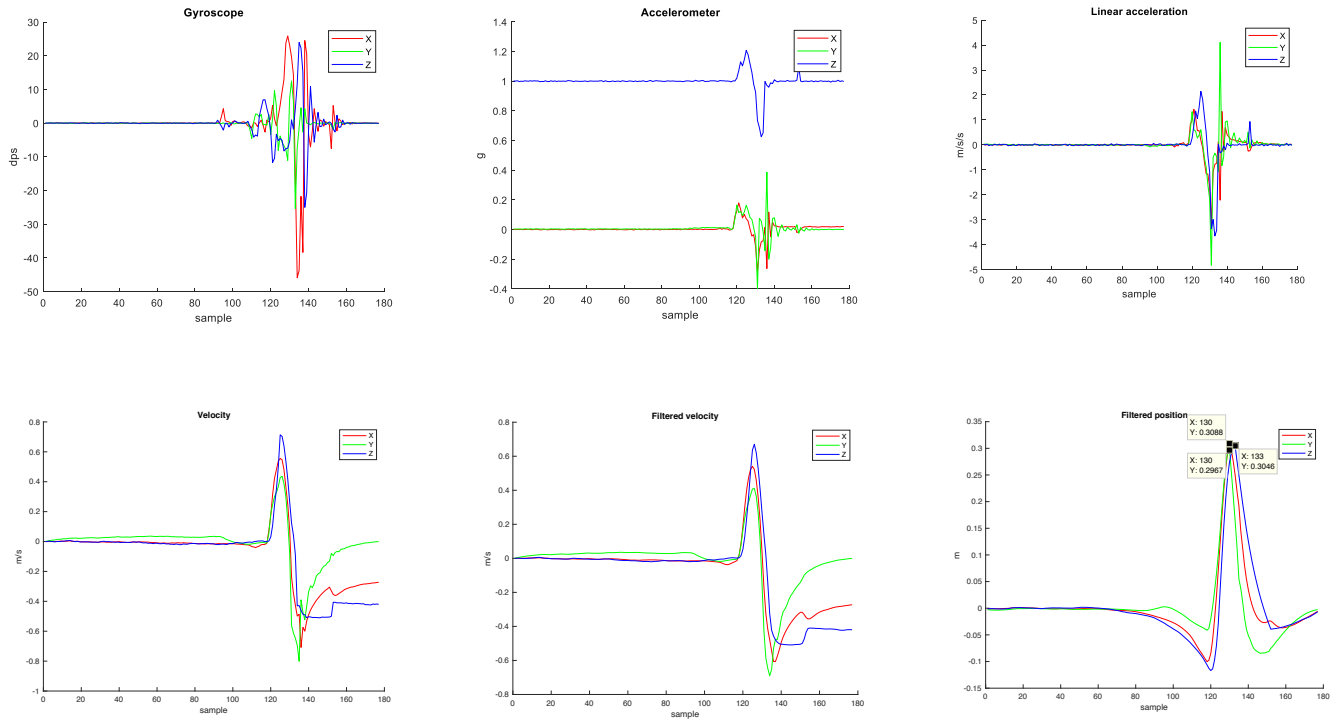


Figure 52 Plots when moving sensors 30cm at X, Y and Z. Lower right the position plot is displayed with the values.

As we can realize, the experiments were done first on each axis separately in order to see how the algorithm works. Then XY axis combined was tested and finally on all three axes. At the next paragraph we will present the accuracy and repeatability of the sensor separately on each axis and combined.

4.2 Accuracy and Repeatability

The accuracy and repeatability of a sensor are the main characteristics in order to define how trustworthy the sensor is. Five experiments were taken on each separate movement of the sensor with the exact same parameters and at the same length on a certain point. Figure 53 shows the results of five experiments taken on X axis after moving the sensor at the exact same point at 60cm.

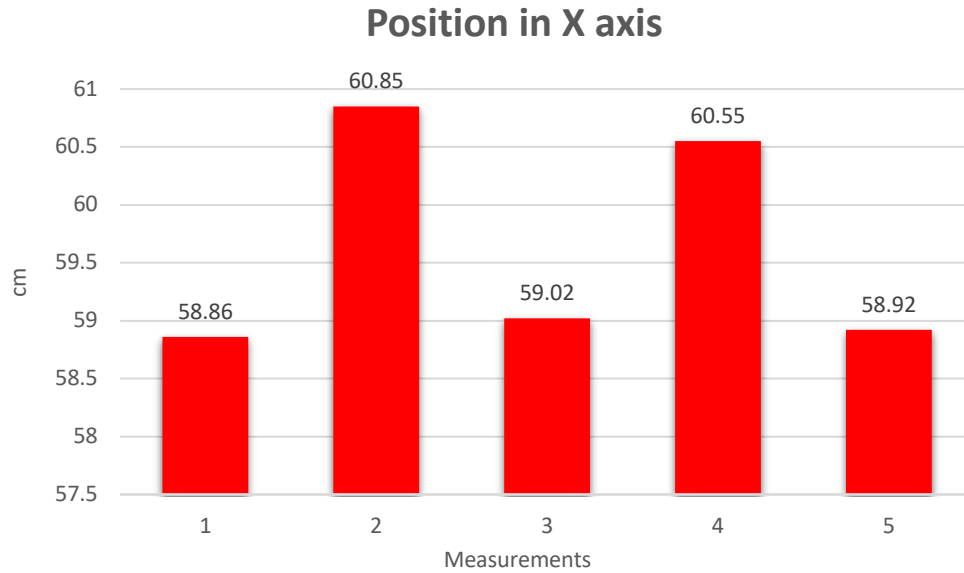


Figure 53 Measurement results when moving sensor at 60cm on X axis

From figure 53 we can calculate the mean accuracy with the following equation:

$$\text{median accuracy}(cm) = \frac{\sum_n |X_{real} - X_{sensor}|}{n}$$

where

X_{real} , is the real value of distance measured in centimeters

X_{sensor} , is the value measured by sensor in centimeters

n , is the total number of measurements

So according to median accuracy equation the result is 0.92cm which means that we have an error of 0.92cm at X axis. From the same figure the repeatability can be also extracted. It is really hard for the sensor to reach the same exact value every time we move it with the exact same parameters in the exact same spot.

Figure 54 shows the result positions of five experiments taken on Y axis after moving the sensor at the exact same point at 60cm.

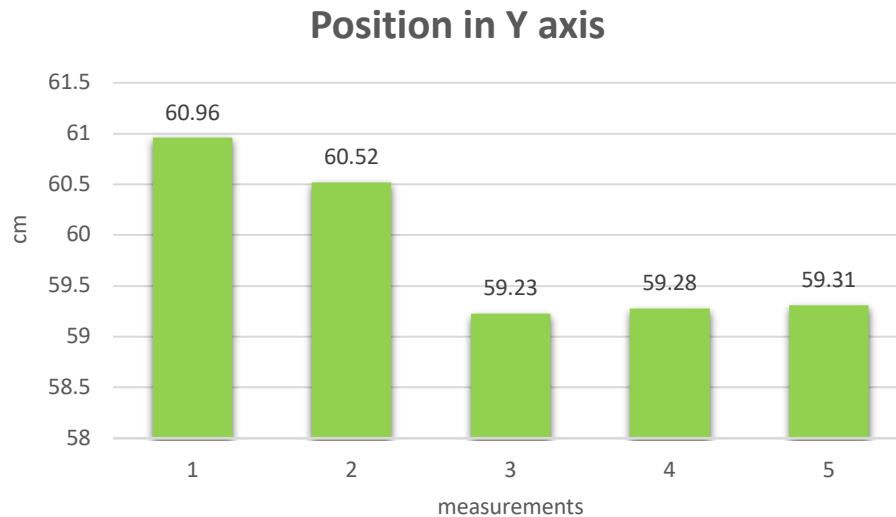


Figure 54 Measurement results when moving sensor at 60cm on Y axis

From median accuracy equation the result is 0,732cm. So, at Y axis we have an error of 0,732cm. Again, we can see that even though we move the sensor at the same spot with the same parameters, it never displays the same value.

Now five experiments are showcased when we move the sensor at 30cm on Z axis. The median accuracy for the results presented in figure 55 was calculated to be 0,794cm while in figure 56 that is a combine movement on X and Y axis at 30cm is 0,942cm for the X axis and for the Y axis is 0,798cm. Finally, in figure 57 we display the results when we move the sensor on all three axes at 30cm, the median accuracy at X is 0,898cm, at Y is 0,898cm as well and at Z is 0,746cm.

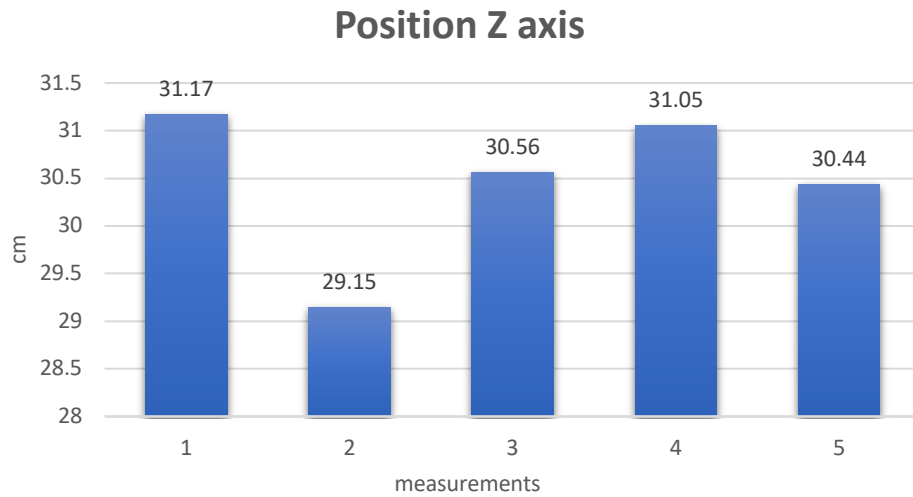


Figure 55 Measurement results when moving sensor at 30cm on Z axis

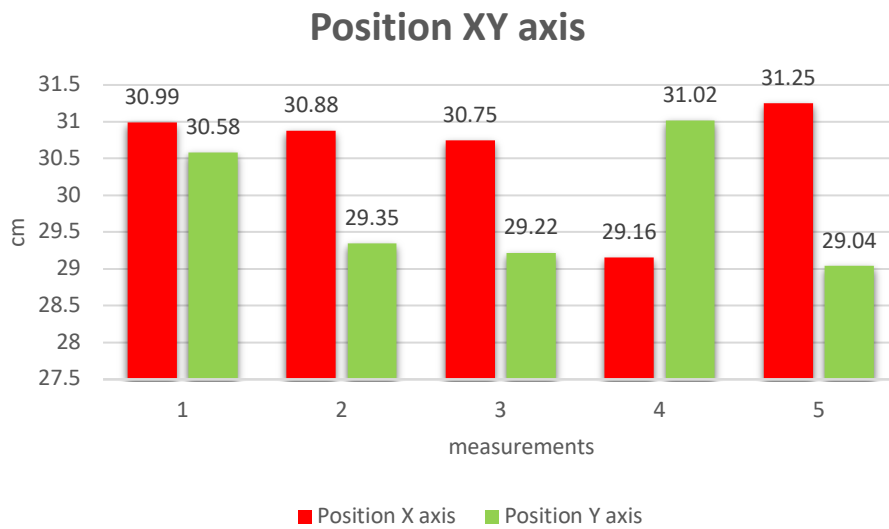


Figure 56 Measurement results when moving sensor at 30cm on X and Y axis

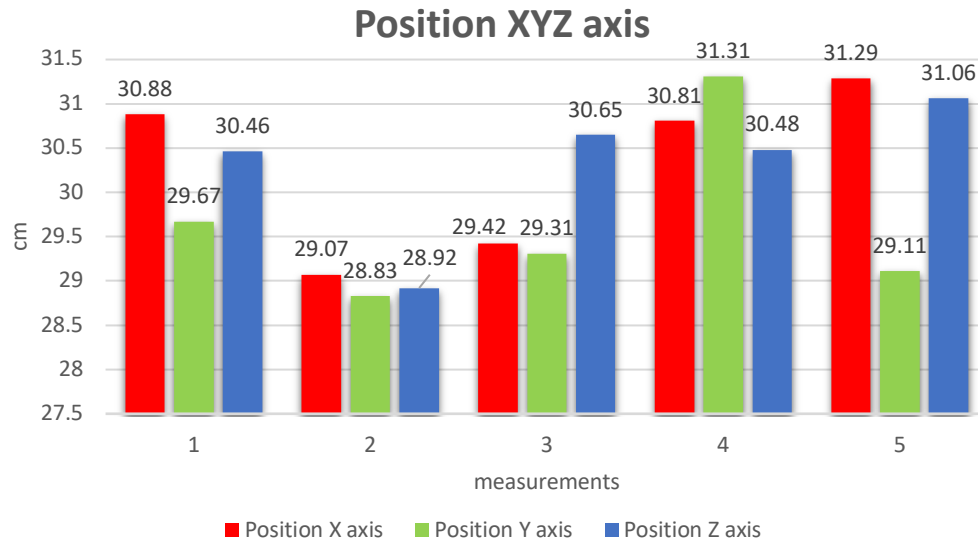


Figure 57 Measurement results when moving sensor at 30cm on X, Y axis and Z axis

So, in table 3 we showcase all the accuracies we calculated from every movement that was tested.

Table 3 Overview of accuracies in each movement that was tested.

Movement	Experiment 1 (cm)			Experiment 2 (cm)			Experiment 3 (cm)			Experiment 4 (cm)			Experiment 5 (cm)			Accuracy (%)			Repeatability(cm) (SD)			
X(60cm)	58,86			60,85			59,02			60,55			58,92			92			0,87			
Y(60cm)	60,96			60,52			59,23			59,28			59,31			73,2			0,73			
Z(30cm)	31,17			29,15			30,56			31,05			30,44			79,8			0,72			
XY(30cm)	30,99		30,58	30,88		29,35	30,75		29,22	29,16		31,02	31,25		29,04	94,2		79,8		0,74		0,8
XYZ(30cm)	30,88	29,67	30,46	29,07	28,33	28,92	29,42	29,31	30,65	30,81	31,31	30,48	31,29	29,11	31,06	89,8	89,8	74,6	0,88	0,98	0,73	

From the result it can be observed that the accuracy remains almost the same when the sensor is moved at a single or multiple axis. Also, from lots of experiments taken it was realized that the sensor has an accuracy error of ± 2 cm. Repeatability was calculated by using the Standard Deviation method.

Chapter 5

Conclusions and Future Work

In this thesis, the development of a very low-cost 3D position system was presented, that was based on system called INS (Inertial Navigation System). By using a sensor called IMU (Inertial Measurement Unit) 3D data of the sensor's position was acquired. According to the experimental results, the proposed system accuracy is acceptable in biomedical applications where inaccuracies will not affect the health of a patient. The cost of the whole system was less than 20 € without including the PC that was used and the software. There is a system done by Memsense Inc. called Nano IMU that cost more than 1300 \$.

The system comes with some limitations, first after many experiments it was realized that the sensor works better if it moves at a medium steady speed and second under no reason the movement of the sensor shall stop, otherwise it will result in huge errors. Finally, the system works for short term period of time, what this means is that the system after a measurement needs to be restarted to get the next measurement.

Position tracking with the use of a low-cost inertial sensor continuous to remain an unsolved problem. Not much research has focused on this topic which means there is plenty of space for several improvements and modifications that can take place. There is a plentiful of hardware and software modifications that can be utilized. For the hardware section, there are many other sensors much better than MPU9250 but with much higher cost, also there many breakout boards containing IMUs (Inertial Measurement Units) that could make many things much easier such as saving the data in a .csv file again the cost increases, an example of such sensor is 9DoF Razor IMU. Regarding to accuracy, even though the software plays a huge part

there is solution by implementing hardware. Such hardware that can increase the accuracy is an UWB (Ultra-Wideband) system that can work in an indoor environment or a GNSS (Global Navigation Satellite System) that functions great at an outdoor environment and much other systems that again increase cost. Also, the system can be more portable, durable and robust by placing it into a box. Concerning the software, to make the system more stable another algorithm can be applied in order to reduce even more the drift and make the system work for longer period of time or updating the current software. One of the most important goal for the future is to make the system work in real time. Also, Kalman filtering, commonly known as linear quadratic estimation, is a way to reduce inaccuracies. With this algorithm, instead of using a single measurement to determine the outcome, series of measurements are observed and processed. The data containing statistical noise or other inaccuracies are analyzed and estimation is produced that is more accurate. To apply the Kalman filter another way of getting the position is needed, such as a GPS.

Bibliography

- [1] L. Horrocks, 23 August 2019. [Online]. Available: <https://www.hotcoursesabroad.com/study-abroad-info/subject-guides/why-study-biomedical-engineering/>. [Accessed 2 October 2019].
- [2] T. GRUJIC, . I. STANCIC and . M. BONKOVIC, "Biomedical Engineering in Practice: Human Motion Tracking, Detection and Analysis," in *Faculty of Electrical Engineering, Mechanical Engineering and Naval Architecture University of Split Rudjera Boskovic* 32 .
- [3] L. Yang, . R. Vyas, A. Rida, J. Pan and M. Tentzeris, "Wearable RFID-Enabled Sensor Nodes for Biomedical Applications," in *58th Electronic Components and Technology Conference*, Atlanta, 2008.
- [4] [Online]. Available: https://en.wikipedia.org/wiki/Positional_tracking.
- [5] [Online]. Available: <https://www.mems-exchange.org/MEMS/what-is.html>. [Accessed 8 January 2020].
- [6] [Online]. Available: <https://www.semiconductorstore.com/blog/2015/What-is-the-Difference-Between-GNSS-and-GPS/1550/> . [Accessed 23 October 2019].
- [7] [Online]. Available: <https://cambridgeic.com/news/newsflash/how-to-select-a-position-sensor>.
- [8] [Online]. Available: https://www.electronics-tutorials.ws/io/io_2.html. [Accessed 25 October 2019].
- [9] P. Kumar, "Interfacing VL6180 ToF Range Finder Sensor with Arduino for Distance Measurement," [Online]. Available: <https://circuitdigest.com/microcontroller-projects/arduino-vl6180-tof-range-finder-sensor-for-distance-measurement>.
- [10] K.-G. Tryfonas, "DEVELOPMENT OF A SENSOR FOR DETECTING THE POSITION OF OBJECTS IN SPACE IN VIRTUAL REALITY APPLICATIONS," Chania , 2016.
- [11] Z. Koppanyi, C. Toth and D. Grejner-Brzezinska, "Positioning in Challenging Environments Using Ultra-Wideband Sensor Networks," 5 March 2015. [Online].

- Available: <https://www.gpsworld.com/innovation-where-are-we/>. [Accessed 8 December 2019].
- [12] E. Dahlgren and H. Mahmood, "Evaluation of indoor positioning based on Bluetooth RSmart technology," in *Master of Science Thesis in the Programme Computer Systems and Networks*, 2014.
- [13] R. Mautz, "Indoor Positioning Technologies," in *Institute of Geodesy and Photogrammetry, Department of Civil, Environmental and Geomatic Engineering*, Zurich, 2012.
- [14] K. Sanford, "Smoothing Kinect Depth Frames in Real-Time," 24 January 2012. [Online]. Available: <https://www.codeproject.com/Articles/317974/KinectDepthSmoothing>. [Accessed 5 December 2019].
- [15] "Learn about Nature," [Online]. Available: <https://www.learnaboutnature.com/animals/bats/bat-ecolocation/>. [Accessed 7 January 2020].
- [16] "Indoor Localization with RFID," infsoft, [Online]. Available: <https://www.infsoft.com/technology/positioning-technologies/rfid>. [Accessed 7 January 2020].
- [17] K. Sidhu, "Understanding Linear Position Sensing Technologies," FierceElectronic, 1 July 2012. [Online]. Available: <https://www.fierceelectronics.com/components/understanding-linear-position-sensing-technologies>. [Accessed 10 January 2020].
- [18] [Online]. Available: <https://www.ceva-dsp.com/ourblog/what-is-an-imu-sensor/>. [Accessed 12 November 2019].
- [19] [Online]. Available: https://en.wikipedia.org/wiki/Inertial_measurement_unit.
- [20] [Online]. Available: <https://enigma2eureka.blogspot.com/2017/10/9-dof-sensor-instead-of-absolute.html>.
- [21] [Online]. Available: http://v-fedun.staff.shef.ac.uk/Integration%20and%20Differential%20Equations/ACS123_lecture_4.html.
- [22] D. H. Titterton and J. L. Weston, "Strapdown Inertial Navigation Technology - 2nd Edition," in *The Institution of Electrical Engineers*.
- [23] D. P. Groves, "NAVIGATION USING INERTIAL SENSORS".

- [24] M. Andrejašic, "MEMS ACCELEROMETERS," *University of Ljubljana Faculty for mathematics and physics Department of physics*, March 2008.
- [25] [Online]. Available: <https://maker.pro/arduino/tutorial/how-to-interface-arduino-and-the-mpu-6050-sensor> . [Accessed 28 October 2019].
- [26] [Online]. Available: <https://howtomechatronics.com/how-it-works/electrical-engineering/mems-accelerometer-gyroscope-magnetometer-arduino/>.
- [27] [Online]. Available: http://wikid.io.tudelft.nl/WikID/index.php/Hall_effect_Magnetometer . [Accessed 5 November 2019].
- [28] [Online]. Available: <http://www.chrobotics.com/library/understanding-euler-angles>. [Accessed 24 November 2019].
- [29] W. R. Hamilton, "ON QUATERNIONS, OR ON A NEW SYSTEM OF IMAGINARIES IN ALGEBRA".
- [30] [Online]. Available: <http://www.chrobotics.com/library/understanding-quaternions>.
- [31] [Online]. Available: https://graphics.fandom.com/wiki/Conversion_between_quaternions_and_Euler_angles.
- [32] [Online]. Available: https://en.wikipedia.org/wiki/Attitude_and_heading_reference_system.
- [33] E. M. Diaz, F. de Ponte Muller, A. R. Jimenez and F. Zampella, "Evaluation of AHRS Algorithms for Inertial Personal Localization in Industrial Environments," in *Industrial Technology (ICIT)*, Seville, Spain, 2015.
- [34] "3.6 Finding Velocity and Displacement from Acceleration," lumencandela, [Online]. Available: <https://courses.lumenlearning.com/suny-osuniversityphysics/chapter/3-6-finding-velocity-and-displacement-from-acceleration/>. [Accessed 11 January 2020].
- [35] O. Maklouf and A. Adwaib, "Performance Evaluation of GPS \ INS Main Integration Approach," *World Academy of Science, Engineering and Technology International Journal of Aerospace and Mechanical Engineering Vol:8, No:2*, 2014.
- [36] "SparkFun IMU Breakout - MPU-9250," sparkfun, [Online]. Available: <https://www.sparkfun.com/products/13762>. [Accessed 12 December 2019].
- [37] "MPU-9250 Product Specification Revision 1.0," InvenSense, 17 January 2014. [Online]. Available: https://cdn.sparkfun.com/assets/learn_tutorials/5/5/0/MPU9250REV1.0.pdf. [Accessed 1 September 2019].

- [38] SparkFun, [Online]. Available: <https://learn.sparkfun.com/tutorials/mpu-9250-hookup-guide>. [Accessed 1 10 2019].
- [39] A. Bhatt, "Understanding the I2C Protocol," ENGINEERSGARAGE, 27 January 2019. [Online]. Available: <https://www.engineersgarage.com/tutorials/understanding-the-i2c-protocol/>. [Accessed 16 November 2019].
- [40] Embedded C, [Online]. Available: <http://www.mbeddedc.com/2017/05/i2c-bus-communication-protocol-tutorial.html>. [Accessed 4 10 2019].
- [41] T. Hamel and R. Mahony, "Attitude estimation on $SO(3)$ based on direct inertial measurements," *Proceedings of the 2006 IEEE International Conference on Robotics and Automation Orlando, Florida*, May 2006.
- [42] R. Mahony, T. Hamel and J.-M. Pflimlin, "Complementary filter design on the special orthogonal group $SO(3)$," *Proceedings of the 44th IEEE Conference on Decision and Control, and the European Control Conference 2005 Seville, Spain*, December 2005.
- [43] M. Euston, P. Coote, R. Mahony, J. Kim and T. Hamel, "A Complementary Filter for Attitude Estimation of a Fixed-Wing UAV".
- [44] [Online]. Available: https://en.wikipedia.org/wiki/Tera_Term.
- [45] S. Sarabandi and F. Thomas, "Accurate Computation of Quaternions from Rotation Matrices," in *Institut de Robòtica i Informàtica Industrial (CSIC-UPC)*, Barcelona, Spain.
- [46] D. P. Jones, *Biomedical Sensors*, New York: MOMENTUM PRESS, 2010.
- [47] M. Kok, J. D. Hol and T. B. Schon, "Using Inertial Sensors for Position and Orientation Estimation".